RADIATION LEAKAGE FROM ACRYLIC ELECTRON CONES FOR AN INTRAOPERATIVE THERAPY LINEAR ACCELERATOR

CHOENGCHAI ORKONGKIAT

A THESIS SUBMITTED IN PARTIAL FULFILLMENT
OF THE REQUIRMENT FOR
THE DEGREE OF MASTER OF SCIENCE
(MEDICAL PHYSICS)
FACULTY OF GRADUATE STUDIES
MAHIDOL UNIVERSITY
2000

ISBN 974-663-815-7

Thesis

entitled

RADIATION LEAKAGE FROM ACRYLIC ELECTRON CONES FOR AN INTRAOPERATIVE THERAPY LINEAR ACCELERATOR

Choengchai Orkongkiat
.....
Mr.Choengchai Orkongkiat
Candidate

Chirapha Tannanonta
.....
Assist. Prof. Chirapha Tannanonta, M.S.
Major advisor

Sivalee Suriyapee
.....
Associate. Prof. Sivalee Suriyapee, M.Eng.
Co-advisor

.....
Prof. Liangchai Limlomwongse, Ph.D.
Dean
Faculty of Graduate Studies

Chirapha Tannanonta
.....
Assist. Prof. Chirapha Tannanonta, M.S.
Chairman
Master of Science Programme
In Medical Physics
Faculty of Medicine,
Ramathibodi Hospital

Thesis

entitled

RADIATION LEAKAGE FROM ACRYLIC ELECTRON CONES FOR AN INTRAOPERATIVE THERAPY LINEAR ACCELERATOR

was submitted to the Faculty of Graduate Studies, Mahidol University
for the degree of Master of Science (Medical Physics)

On
May 19, 2000

Choengchai Orkongkiat
.....
Mr.Choengchai Orkongkiat
Candidate

C. Wongket
.....
Associate. Prof. Chavalit Wongse-ek, M.Sc.
Member

Chirapha Tannanonta
.....
Assist. Prof. Chirapha Tannanonta, M.S.
Chairman

Ratana Pirabul
.....
Assist. Prof. Ratana Pirabul, M.Sc.
Member

Sivalee Suriyapee
.....
Associate. Prof. Sivalee Suriyapee, M.Eng.
Member

Liangchai Limlomwongse
.....
Prof. Liangchai Limlomwongse, Ph.D.
Dean
Faculty of Graduate Studies
Mahidol University

Prakit Vathesatogkit
.....
Prof.Prakit Vathesatogkit, M.D.
A.B.I.M.
Dean
Faculty of Medicine,
Ramathibodi Hospital
Mahidol University

ACKNOWLEDGEMENT

I would like to express my sincere gratitude and deep appreciation to Asst. Prof. Chirapa Tannanonta, my major advisor for the suggestion, helpful advice, comments, reviewing and correcting for this thesis. I am equally grateful to my co-advisor Assoc. Prof. Sivalee Suriyapee from the Department of Radiology, Faculty of medicine, Chulalongkorn Hospital for the suggestion, guidance, and constructive comments for this thesis. They are very nice and kindness.

A special gratitude is expressed to Prof. Puangtong Kraipibul MD., head of the Department of Radiology, Ramathibodi Hospital, for her supporting on the use of the equipments in the department.

I would like to thank Assist. Prof. Ratana Pirabul, all staffs and colleagues in the school of Medical Physics for supplying me the academic knowledge in Medical Physics.

I would like to thank Assoc. Prof. Chavalit Wongse-ek, from the Faculty of medical technology, Mahidol University for the suggestion, guidance, and constructive comments for this thesis.

I would like to thank Assist. Prof. Duangpen Poochinda, Assoc. Prof. Dr. Vipa Boonkitticharoen for their willpower and kindness.

Finally, I would like to mention immeasurable contribution and encouragement of my father and mother. I will tell them that "I can do it".

Choengchai Orkongkiat

3936131 RAMP/M : MAJOR : MEDICAL PHYSICS ; M.Sc.(MEDICAL PHYSICS)
KEY WORDS : IORT / RADIATION LEAKAGE / LINEAR ACCELERATOR / TLD / FILM

CHOENGCHAI ORKONGKIAT : RADIATION LEAKAGE FROM ACRYLIC ELECTRON CONES FOR AN INTRAOPERATIVE THERAPY LINEAR ACCELERATOR. THESIS ADVISORS : CHIRAPHA TANNANONTA, M.S.,SIVALEE SURIYAPEE, M.Eng. 122 P. ISBN 974-663-815-7

In an intraoperative radiation treatment (IORT), normal tissues may be adjacent to the outer wall of the treatment cone. It is very important to determine the leakage radiation outside the cone wall in addition to the beam data since a large single dose is delivered to the tumor.

In this study, radiographic films were wrapped around the cone wall to locate the area of the high radiation leakage according to the optical density of the films. Then the leakage doses at the cone wall with high optical density starting from the distance of 0-8 cm from the cone end and the dose at the depth of the maximum dose (d_{max}) were measured by using thermoluminescent dosimeters (TLDs). The measurements were made for 4.5, 6.4, 8.3, and 9.5 cm diameter cones (both flat and bevel ends), each with 6, 12, and 20 MeV electron beams. The leakage dose as the percentage of the maximum dose in phantom tended to increase with the energy and cone size except the 8.3 cm cone which showed more leakage than the 9.5 cm cone. For the same cone size and energy, all bevel end cones showed higher leakage dose than the flat ones with the maximum value of 3.95% of the tumor dose for 4.5 cm cone of 20 MeV. The maximum leakage dose for the distance of 4 cm from the cone end was 20.94% of the dose at the depth of maximum dose (d_{max}) with the 8.3 cm bevel end cone for 20 MeV. Normally, the normal tissue adjacent to the cone wall do not extend to more than 4 cm from the end of the cone. So, for the IORT applicating system of Ramathibodi Hospital, the normal tissues should not receive more than 23.10% of the tumor dose if the treatment depth of 90% depth dose is used. The tolerance dose for the normal tissue involved in each treatment should be considered together with the maximum radiation leakage for the cone size and energy used in the treatment.

3936131 RAMP/M : สาขาวิชา : ฟิสิกส์การแพทย์ ; วท.ม. (ฟิสิกส์การแพทย์)

เชิงชาย อ.ก้องเกียรติ : รังสีรั่วไหลจากโคนชนิดอะไครลิคที่ใช้ในการรักษาด้วยลำรังสีอิเลคตรอนจากเครื่องเร่งอนุภาคขณะทำการผ่าตัด. (RADIATION LEAKAGE FROM ACRYLIC ELECTRON CONES FOR AN INTRAOPERATIVE THERAPY LINEAR ACCELERATOR) คณะกรรมการควบคุมวิทยานิพนธ์ : จีระภา ตันนานนท์, M.S., ศิวลี สุริยาปี, M.Eng. 122 หน้า. ISBN 974-663-815-7

ในการรักษาด้วยรังสีขณะทำการผ่าตัดนั้น นอกจากข้อมูลของลำรังสีที่จำเป็นในการรักษาผู้ป่วยแล้ว การหาค่าของปริมาณรังสีรั่วไหลด้านนอกผนังของโคนเป็นสิ่งสำคัญมาก เนื่องจากปริมาณรังสีที่ฉายให้กับก้อนเนื้องอกนั้นจะให้ครั้งเดียวเป็นปริมาณมาก จึงต้องประเมินปริมาณรังสีของเนื้อเยื่อปกติที่อาจอยู่ชิดติดกับผนังด้านนอกของโคนที่ใช้ในการรักษาด้วยว่าได้รับรังสีเกินปริมาณที่เนื้อเยื่อนั้นสามารถทนได้หรือไม่

ในการศึกษาเพื่อตรวจวัดปริมาณรังสีรั่วไหลจากโคนขนาด 4.5, 6.4, 8.3, และ 9.5 เซนติเมตรทั้งปลายตรงและปลายเฉียง สำหรับพลังงานของอิเลคตรอนเท่ากับ 6, 12, 20 เมกกะอิเลคตรอนโวลท์นั้น ทำโดยนำฟิล์มถ่ายภาพทางรังสีชนิดบรรจุในซองกระดาษมาหุ้มรอบโคนเพื่อหาตำแหน่งที่มีรังสีรั่วไหลมากที่สุดในแต่ละระยะจากปลายโคนถึงระยะ 8 เซนติเมตรสูงจากปลายโคน จากความดำบนฟิล์มเมื่อได้ตำแหน่งที่มีรังสีรั่วไหลสูงตามระยะต่างๆแล้วจึงใช้ตัววัดรังสีเทอร์โมลูมิเนสเซ็นต์วางที่ตำแหน่งเหล่านั้นและวางที่ความลึกที่มีปริมาณรังสีมากที่สุดภายในแฟนทอมด้วยเพื่อวัดปริมาณรังสีเป็นเกรย์ ผลการวัดปริมาณรังสีรั่วไหลเทียบเป็นเปอร์เซ็นต์ของปริมาณรังสีสูงสุดในแฟนทอมจะเพิ่มขึ้นตามพลังงานและขนาดของโคน ยกเว้นโคนขนาด 8.3 เซนติเมตรซึ่งมีค่าของรังสีรั่วไหลมากกว่าโคนขนาด 9.5 เซนติเมตร ที่ขนาดโคนและพลังงานเท่ากันโคนปลายเฉียงมีรังสีรั่วไหลมากกว่าโคนปลายตรงด้วยค่าสูงสุดเท่ากับ 3.95 เปอร์เซ็นต์ของรังสีที่ก้อนเนื้องอกจากโคนขนาด 4.3 เซนติเมตรกับพลังงาน 20 เมกกะอิเลคตรอนโวลท์ เมื่อพิจารณาถึงปริมาณรังสีรั่วไหลสูงสุดสำหรับระยะ 4 เซนติเมตรจากปลายโคนพบว่าโคนปลายเฉียงขนาด 8.3 เซนติเมตรที่พลังงาน 20 เมกกะอิเลคตรอนโวลท์ แสดงค่าสูงสุดเท่ากับ 20.94 เปอร์เซ็นต์ของปริมาณรังสีสูงสุดในแฟนทอม โดยทั่วไปแล้วเนื้อเยื่อปกติที่อยู่ติดผนังของโคนจะไม่ยื่นสูงขึ้นมาเกิน 4 เซนติเมตร จากปลายโคน ดังนั้นในการรักษาด้วยรังสีขณะทำการผ่าตัดด้วยอุปกรณ์ของโรงพยาบาลรามาธิบดีนั้นปริมาณรังสีที่เนื้อเยื่อปกติจะได้รับไม่ควรเกิน 23.10 เปอร์เซ็นต์ของปริมาณรังสีที่ให้กับเนื้องอกที่ความลึก 90 เปอร์เซ็นต์ของปริมาณรังสีสูงสุด เมื่อทราบค่าปริมาณรังสีที่เนื้อเยื่อปกติแต่ละชนิดจะทนได้ จะสามารถพิจารณาว่าเนื้อเยื่อปกตินั้นจะได้รับปริมาณรังสีเกินที่จะทนได้หรือไม่สำหรับการรักษาเนื้องอกแต่ละครั้งนั้นจากปริมาณรังสีรั่วไหลที่วัดได้ของแต่ละโคนและพลังงานที่ใช้รักษาจริงที่ได้ทำการวัดไว้ล่วงหน้าแล้ว

LIST OF CONTENTS

	Page
ACKNOWLEDGEMENT	iii
ABSTRACT	iv
LIST OF CONTENTS	vi
LIST OF TABLES	vii
LIST OF FIGURES	ix
LIST OF ABBREVIATIONS	xii
CHAPTER	
I INTRODUCTION	1
1.1 LINEAR ACCELERATOR	3
1.2 ELECTRON INTERACTIONS WITH MATTER	6
1.3 BASIC PARAMETERS OF ELECTRON BEAMS	9
1.4 THE IORT TREATMENT FACILITY	14
1.5 THERMOLUMINESCENT DOSIMETRY	31
1.6 FILM DOSIMETER	36
II OBJECTIVES	38
III LITERATURE REVIEW	39
IV MATERIALS AND METHODS	41
4.1 MATERIALS	41
4.2 METHODS	48
V RESULTS	55
VI DISCUSSION	101
VII CONCLUSION	102
REFERENCES	104
BIOGRAPHY	109

LIST OF TABLES

		Page
Table I	The optical density of radiographic film at various points on the cone surface starting from the cone end of the cone diameter 4.5 cm with flat end for electron beam 6, 12, and 20 MeV.	58
Table II	The optical density of radiographic film at various points on the cone surface starting from the cone end of the cone diameter 4.5 cm with bevel end for electron beam 6, 12, and 20 MeV.	61
Table III	The optical density of radiographic film at various points on the cone surface starting from the cone end of the cone diameter 6.4 cm with flat end for electron beam 6, 12, and 20 MeV.	64
Table IV	The optical density of radiographic film at various points on the cone surface starting from the cone end of the cone diameter 6.4 cm with bevel end for electron beam 6, 12, and 20 MeV.	67
Table V	The optical density of radiographic film at various points on the cone surface starting from the cone end of the cone diameter 8.3 cm with flat end for electron beam 6, 12, and 20 MeV.	70
Table VI	The optical density of radiographic film at various points on the cone surface starting from the cone end of the cone diameter 8.3 cm with bevel end for electron beam 6, 12, and 20 MeV.	76

LIST OF TABLES (continued)

		Page
Table VII	The optical density of radiographic film at various points on the cone surface starting from the cone end of the cone diameter 9.5 cm with flat end for electron beam 6, 12, and 20 MeV.	82
Table VIII	The optical density of radiographic film at various points on the cone surface starting from the cone end of the cone diameter 9.5 cm with bevel end for electron beam 6, 12, and 20 MeV.	88
Table IX	The depth of maximum dose in water phantom of IORT cone diameters 4.5, 6.4, 8.3, and 9.5 cm for electron beam energies of 6, 12, and 20 MeV both flat and 30° beveled ends.	94
Table X	The maximum radiation leakage in the percentage of dose at d_{max} of IORT cone measured by TLDs.	95
Table XI	The leakage dose at the distance of 4 cm from the cone end in the percentage of the value at dmax for the various sizes of the cones and energies.	100
Table XII	The leakage dose at the distance of 4 cm from the cone end as the percentage of the tumor dose at the treatment depth of 90% isodose.	100

LIST OF FIGURES

	Page
Figure 1. The block diagram of a medical linear accelerator.	3
Figure 2. Basic electron interaction processes.	6
Figure 3. The distribution for energy fluence, Φ_E, of an electron beam as passing through the collimation system of the accelerator and the phantom.	9
Figure 4. Central axis depth dose curve of an electron beam showing the parameters required for clinical treatment.	11
Figure 5. Central axis depth dose curves of various electron beam energies.	11
Figure 6. Isodose chart of an electron beams.	12
Figure 7. Hard docking IORT system (side lateral docking type).	16
Figure 8. The transparent applicators of Ramathibodi hospital.	17
Figure 9. The difference width of the brass plate on the top of different cone diameter.	17
Figure 10. Hard docking IORT system (vertical slide docking type).	19
Figure 11. Three possible configurations for defining the central axis of bevel end applicator.	22
Figure 12. The dose distribution for 15 MeV electron beam of flat end and 15° bevel end applicator with chosen the second configuration.	23
Figure 13. The %DD value along the beam axis compare with the %DD value along the tumor axis.	24

LIST OF FIGURES (continued)

Page

Figure 14. The dose distribution for 15 MeV electron beam of 15° and 30° bevel end applicator with chosen the third configuration. 25

Figure 15. Beam profile of 18 MeV electron beam for 3.5 inches with 30° bevel end applicator. 27

Figure 16. Percent horn relative to dose on central axis plotted as a function of energy for 3.5 inches flat end applicator. 28

Figure 17. Percent penumbra outside the useful beam of 15° bevel angle Applicator plotted as a function of electron beam surface energy. 29

Figure 18. Diagram showing apparatus for measuring light output from a thermoluminescent material. 32

Figure 19. Glow curve for a thermoluminescent material showing relative light output as a function of heating time. 33

Figure 20. The characteristic curve of a film exposed to a 10 MeV electron beam. 37

Figure 21. The linear accelerator with RFA300 Radiation Field Analyzer. 43

Figure 22. Automatic thermoluminescent dosimeter reader. 45

Figure 23. Film densitometer. 46

Figure 24. The irradiation technique in the determination of the maximum leakage outside an IORT cone by using a radiographic film. 49

Figure 25. The irradiation technique for leakage measurements by using thermoluminescent dosimeters (TLDs). 53

LIST OF FIGURES (continued)

Page

Figure 26. The percent of radiation leakage related to the dose at the depth of maximum dose as a function of the distance(cm) from the cone end for 4.5 cm diameter cone with flat end and bevel ends. 96

Figure 27. The percent of radiation leakage related to the dose at the depth of maximum dose as a function of the distance(cm) from the cone end for 6.4 cm diameter cone with flat end and bevel ends. 97

Figure 28. The percent of radiation leakage related to the dose at the depth of maximum dose as a function of the distance(cm) from the cone end for 8.3 cm diameter cone with flat end and bevel ends. 98

Figure 29. The percent of radiation leakage related to the dose at the depth of maximum dose as a function of the distance(cm) from the cone end for 9.5 cm diameter cone with flat end and bevel ends. 99

LIST OF ABBREVIATIONS

Abbreviations	Term
Al	Aluminum
°C	Degree Celsius
D	actual exposure
cGy	centigray
cm	centimeter
%DD	percentage depth dose
d_{max}	depth of maximum dose
ECC	Element correction coefficient
g	gram
Gy	Gray
keV	kiloelectron volt
L	calibration absorbed dose
LiF	Lithium Fluoride
MeV	megaelectron volt
μGy	microgray
mGy	milligray
mm	millimeter
MV	megavolt
nC	Nanocoulomb

LIST OF ABBREVIATIONS (Continued)

Abbreviations	Term
OD	optical density
Pb	Lead
PC	Personal computer
PMT	Photomultiplier tube
ppm	part per million
Q	charge integral
R	Roentgen
RCF	Reader Calibration Factor
RF	Radiofrequency wave
RFA	Radiation Field Analyzer
SSD	Source-surface distance
TSD	Target to skin distance
TLD	Thermoluminescent dosimeter
Z	atomic number
Z_{eff}	effective atomic number

CHAPTER I

INTRODUCTION

Intraoperative radiation therapy (IORT) is a cancer treatment which combines two treatment methods, surgery and radiation therapy. The aim of IORT is to give a large single dose to the tumor site, while minimizing the direct or scatter dose to the surrounding healthy tissue. The IORT treatment is given to a patient directly during surgical procedure to expose unresectable neoplasm or the bed of a resected tumor after moving the critical structures from the path of radiation beam. Abe et al (1) defined the IORT as a treatment modality in which surgery will remove the resectable lesion and then the remaining tumor beds will be irradiated by radiation during the surgical procedure. Although an orthovoltage x-ray machine can be used for IORT (2), the most common modality is the use of an electron beam from a linear accelerator with the energies of 6 MeV to 22 MeV (3-6). The orthovoltage unit has an advantage in being less expensive but significant disadvantages in inhomogeneous dose delivery across the tumor volume due to an exponential absorption in tissue and increasing bone absorption by photoelectric absorption process. The IORT treatment has been developed all the time from the past. Until 1964, Abe and co-workers (7) used a megavoltage machine for IORT that was the beginning of modern IORT. The advantage of megavoltage radiotherapy is that it can give a sufficient dose to any location in body. They reported that IORT treatment with electron beam is the best, because the characteristic of electron beam is proper for IORT treatment. The electron

beam energy can be chosen for desired depth of tissue penetration (7). After the desired depth, radiation dose will fall off rapidly with increasing depth, so the problem that normal tissues beneath tumor will be exposed is negligible. This new form of radiotherapy also gives the curative treatment of radioresistance tumors without affecting normal structure, such as skin. In Ramathibodi hospital, IORT with 6-20 MeV electron beams has been used in treating cancer patients since 1997. In the IORT treatment, the normal tissue is frequently very close or contact with the end of the treatment cone and some parts outside the cone wall. For patient safety, the maximum leakage radiation from the IORT cone system which may contribute to the normal tissue of the patient should be measured.

1.1 Linear accelerator

The linear accelerator (LINAC) is a machine that uses high-frequency electromagnetic waves to accelerate electron to high energy for high energy electron beam or accelerate electron to strike a target to produce high energy x-rays. The high energy electron beam can be used for treating superficial tumors and the high energy photon beam used for treating deep-seated tumors. The major component and auxiliary systems for a medical linear accelerator are illustrated in Figure 1.

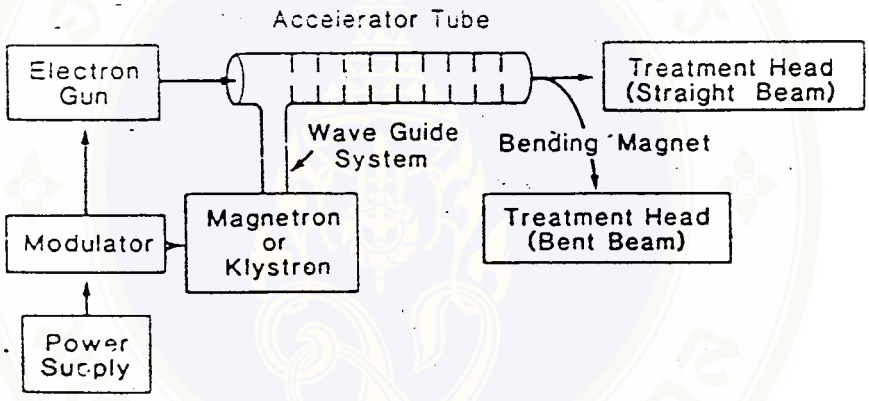

Figure 1. The block diagram of a medical linear accelerator (8).

A power supply provides DC power to the modulator, which includes the pulse-forming network and a switch tube known as hydrogen thyratron. High-voltage pulses from the modulator section are flat-topped DC pulses of a few microseconds in duration. These pulses are delivered to the magnetron or klystron and simultaneously to the electron gun. The magnetron and klystron are used for generating microwaves (8, 9). These pulsed microwave are injected into the accelerator tube via a wave guide system. Electron gun will produce the proper instant electrons which are also pulse injected into the accelerator tube. The accelerator tube is evacuated to a high vacuum.

As the electrons are injected into the accelerating tube, they will interact with electromagnetic field of the microwaves and gain energy from the sinusoidal electric field by an acceleration process. The acceleration process of the medical linear accelerator have two different types by traveling electromagnetic wave or by standing electromagnetic wave (9). As the high energy electrons emerge from the exit window of the accelerating tube, they are in the form of a pencil bean about 3 mm diameter(8). For the linear accelerators with low energy (up to 6 MV), the electrons are allowed to go straight on and strike a target for x-ray production or strike an electron scattering foil for electron beam treatment. In the higher energy linacs, the electrons are bent through a suitable angle (usually about 90° or 270°) between accelerator structure and the target. Since their accelerator structures are too long and, therefore, are placed horizontally or at an angle with respect to the horizontal.

The treatment head contains with x-ray target, scattering foil, flattening filter, ion chamber, fix and movable collimators, and light localizer system. Its head consists of a thick shell of high-density shielding material such as lead, tungsten or lead-tungsten allowed to provide the sufficient shielding of leakage radiation and radiation protection (9).

A fixed primary collimator located beyond the x-ray target is used for first collimation of x-ray beam. The flattening filter is usually made of lead, tungsten, uranium, steel or aluminum. It is usually inserted in the x-ray beam to make the beam intensity uniform across the field because the x-ray intensity of the linear accelerator is peaked in the forward direction. In electron mode, the scattering foil is moved in the radiation beam instead of the flattening filter. After the radiation passes through the flattening filter or the scattering foil, it will incident on the monitoring system

which consists of single or several transmission type ion chamber for example flat parallel plate chamber or cylindrical thimble chamber. The ion chamber is used for monitoring the dose rate, integrated dose, and field symmetry. Beyond the ion chambers is the movable x-ray collimator. It consists of two pairs of lead or tungsten block (jaws) which provide a rectangular opening from 0x0 cm to 40x40 cm of the field size that projected on standard distance such as 100 cm from focal spot of the x-ray target. Light localizing system consists of a light source and a mirror. It is used to provide the field size definition that is congruent with the radiation field.

Both x-ray and electron beams may be available in a linear accelerator or separated ones.

1.1.1 The x-ray beam from linear accelerators

When the electrons incident on a target of high Z material such as tungsten, x-rays are produced. Since the electrons used to produce x-rays are in the megavoltage range, the x-ray intensity is peaked in the forward direction. A flattening filter is inserted in the beam to make the beam intensity uniform across the field.

1.1.2 The electron beam from linear accelerators

For the electron mode, the narrow pencil electron beam exiting the window of the accelerator tube, instead of striking the target, is made to strike an electron scattering foil. The scattering foil will spread the beam and also make the electron fluence be uniform across the treatment field. The scattering foil consists of a thin metallic foil with the suitable thickness for scattering electrons instead of producing bremsstrahlung as x-ray contamination of the electron beam. In some linear accelerators, an electromagnetic scanning may be used to spread the electron pencil beam over a large area instead of using the scattering foil (8, 9).

1.2 Electron interactions with matter

In radiation dosimetry, the mechanism of energy deposition in matter by the radiation field is primary interest. Electron beam as a charge particle, loses energy in a way which is explicitly different from that of a photon beam. Photons need to transfer energy to electrons first before any transfer of energy from the beam can take place. But the electron beams start losing energy immediately to the medium. In the energy range of interest in radiation therapy, the interactions with matter of the electron beams result in direct energy losses or scattering or a combination of both.

1.2.1 Energy losses of electrons

In passing through a medium, the electron losses energy in the medium as an absorbed dose by two principle processes, collisional losses and radiative losses. The difference between these two processes is that the collisional loss involves the outer atomic electrons while the radiative losses involve the atomic nucleus (10) as shown in Figure 2.

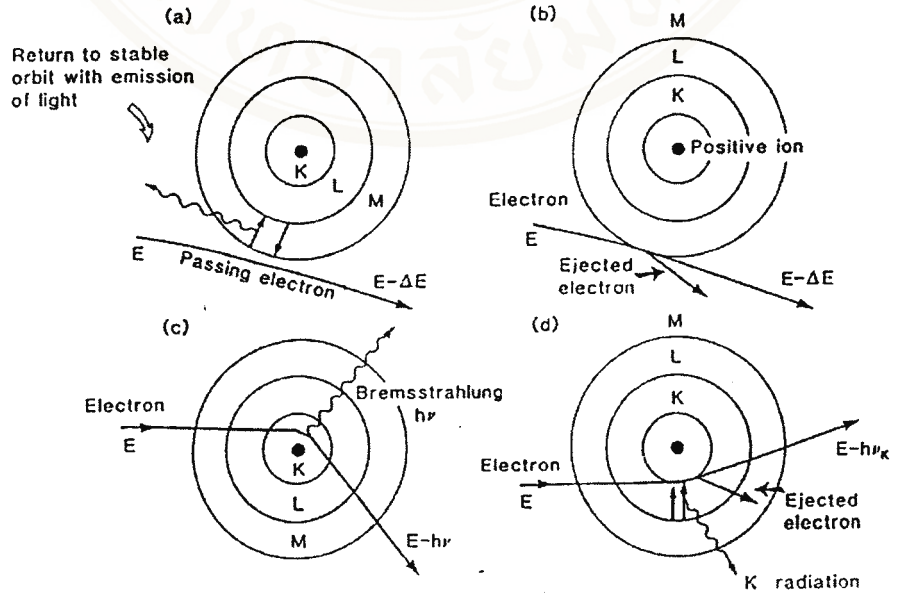

Figure 2. Basic electron interaction processes : (a) excitation, (b) ionization, (c) bremsstrahlung production, (d) characteristic radiation production (10).

1.2.1.1 Collisional energy losses

The electron may have collisional energy losses in either process with excitation or ionization. The probability for any of these processes to take place depends upon the energy of the passing electron, the distance of closest approach, and the atomic number of the medium. The excitation (Figure 2a) will occur if the distance of closest approach to the atom of the passing electron is large compared with the dimensions of the atom. During the excitation, an electron from an inner shell is moved to an outer orbit by a small energy loss. The atom does not remain in excited state very long, it soon de-excites back to the lower state with the emission of the excess energy in the form of electromagnetic radiation. If the medium is gas, the emitting electromagnetic radiation is in the form of visible or ultra-violet light, and in the form of heat or infrared radiation for liquid or solid medium. When the distance of closest approach is closer and the incident electron has enough energy to overcome the binding energy of the orbital electron, this electron is removed from the shell and the atom becomes ionized (Figure 2b).

1.2.1.2 Radiative energy losses

When the distance of the closest approach is smaller than the atomic radius, the collision between the passing electron and an atom is radiative collision (figure 2c). The incident electron will be under influence of the Coulomb field of the nucleus and then deflected (scattered) from its original path with loss of energy. The loss of energy will be emitted in the form of an electromagnetic radiation known as bremsstrahlung with energy hν. Occasionally, with low probability, the passing electron may interact with an atomic electron, e.g., in the K-shell, and the characteristic K-radiation will be emitted as shown in Figure 2d. The angular

distribution of the produced bremsstrahlung is important. For low incident electron energy ($E << mc^2$) as in conventional x-ray tubes, the maximum intensity of the x-rays is perpendicular to the direction of the electron motion. At high energies ($E >> mc^2$), the average angle of emission of a quantum coincides with the direction of motion of the incident electron (10).

1.2.2 Scattering process

Apart from energy losses of electrons, another important aspect of the interaction of electrons with atoms is the change of direction of the electron path. Two types of collisions contribute to scattering: interactions of the passing electron with the Coulomb field of the nucleus and interactions of the passing electron with the orbital electrons (10, 11). In a material with thin layer, the result of any of these collisions is mostly in large angle electron deflection. With a thick layer material, multiple collisions have more opportunity to occur. The result of each collision is a random change of direction of electron, not necessary in the same direction. The net change eventually seen is a small angle deflection. Distributed among the small-angle deflection is an occasional large-angle scattering, which gives rise to an ejection of a δ-ray in the case of an electron-electron collision. The scattering crossections of both types of collisions are large and concentrated in the forward directions with a large number of small-angle scattering collisions. Since the mass of the target nucleus is much greater than that of the electron, the energy transfer of the Coulomb scattering in the most cases is negligible.

1.3 Basic parameters of electron beams

1.3.1 Energy parameters of electron beams

At the end of the accelerating system, the energy of the beam is maximum. Figure 3 illustrates the energy parameters in relation to the points at exit window, at phantom surface, and at a depth in phantom. The parameters for energy distribution with E_m, E_p, E, and T are the maximum energy, the most probable energy, the mean energy, and the energy spread of the spectrum respectively. Additional subscripts referred to the accelerator's window (a), the phantom surface (o), and the depth in the phantom (z) are added to these parameters. The peak energy at the accelerator exit window, $E_{p,a}$, is usually refereed to as the "accelerator energy" or the "nominal accelerator energy".

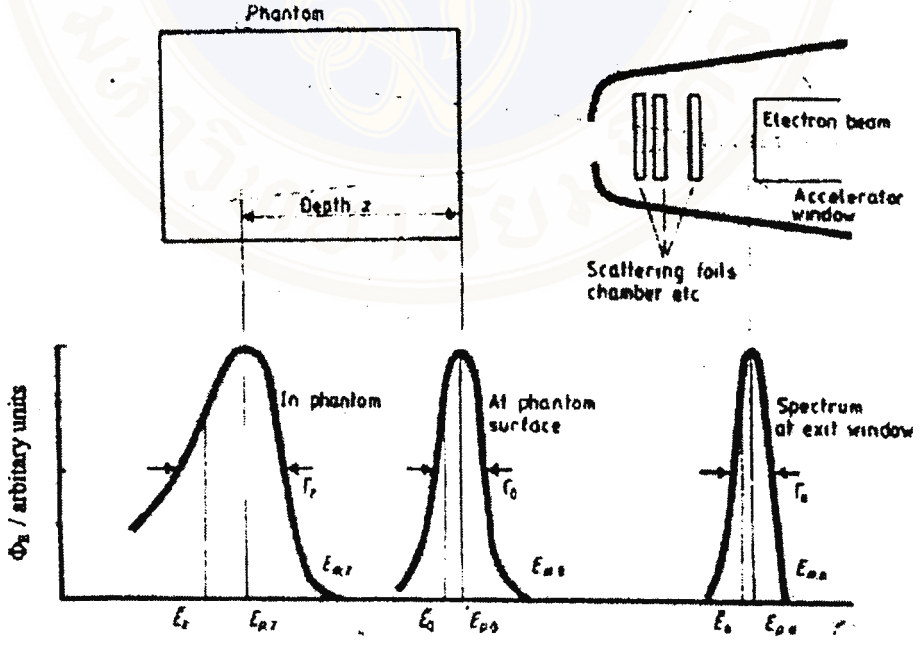

Figure 3. The distribution for energy fluence, Φ_E, of an electron beam as passing through the collimation system of the accelerator and the phantom (12).

1.3.2 Characteristics of clinical electron beams

1.3.2.1 Central axis depth dose curves

The central axis depth dose curve of an electron beam as shown in Figure 4 is obtained by measuring the radiation dose along the central axis of the beam as a function of depth in a homogeneous unit density phantom. The major attraction of the electron beam is the shape of the depth dose curve that has a moderately flat plateau in the first few centimeters of the phantom or tissue, followed by a rapid decreasing to a low dose background produced by the bremsstrahlung x-rays generated in the scattering foil, the collimating system and the irradiated medium. The bremsstrahlung component increases with energy (13). The depth of 90% depth dose is generally taken to be the treatment depth or therapeutic range and can be roughly estimated in centimeters of water or soft tissue as one-third of the mean energy at the phantom surface in MeV. Figure 5 shows the central axis depth dose curves for 4-32 MeV. The central axis depth dose curves become less steep when the electron beam energy increases. The entrance or surface dose stated at 0.5 mm depth increases with increasing energy and it is usually in the range of 80-95% (13). The variation of the depth of peak or maximum dose (Z_m) with the energy is not linear.

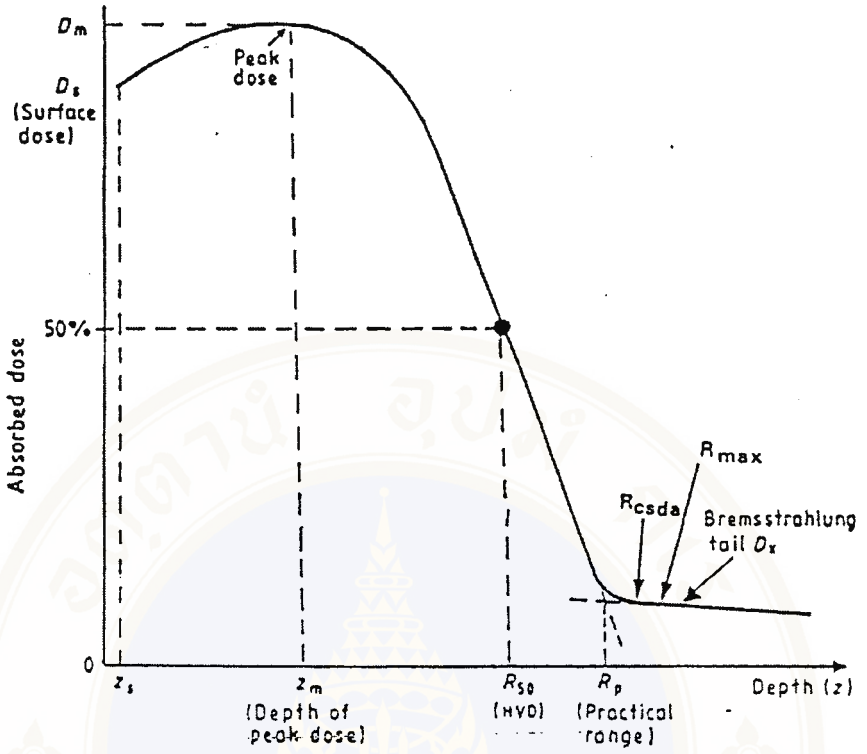

Figure 4. Central axis depth dose curve of an electron beam showing the parameters required for clinical treatment. D_m is the maximum absorbed dose (14).

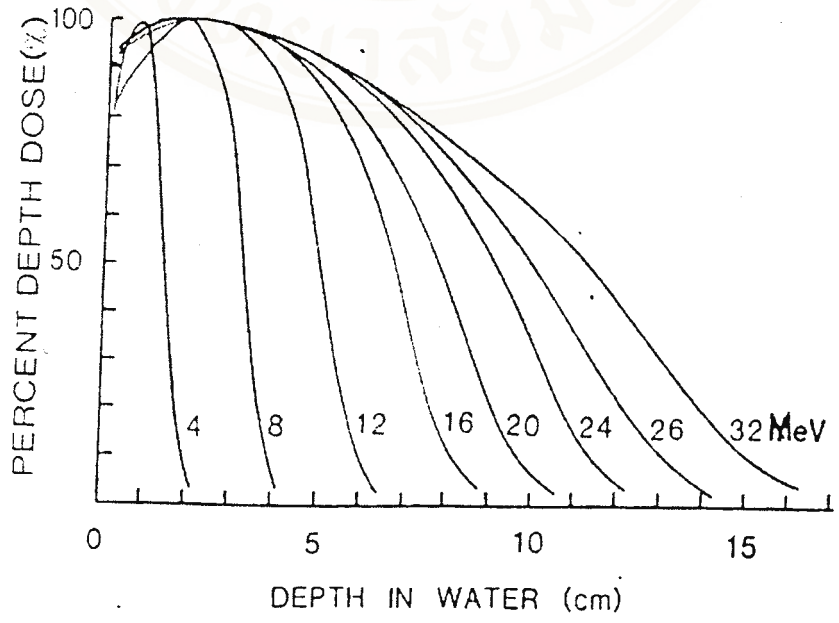

Figure 5. Central axis depth dose curves of various electron beam energies (15).

1.3.2.2 Isodose curves

Figure 6 shows the isodose chart of an electron beam. The electron beam expands rapidly below the surface due to the scattering. At depth, the lower value isodose lines bulge significantly outwards as the higher value isodose lines are pull in. Consequently, the width of high dose volume is reduced as depth increases and can be much narrower at the treatment depth than at the surface. The spread of isodose curves varies, depending on the isodose level, energy, field size, and collimation.

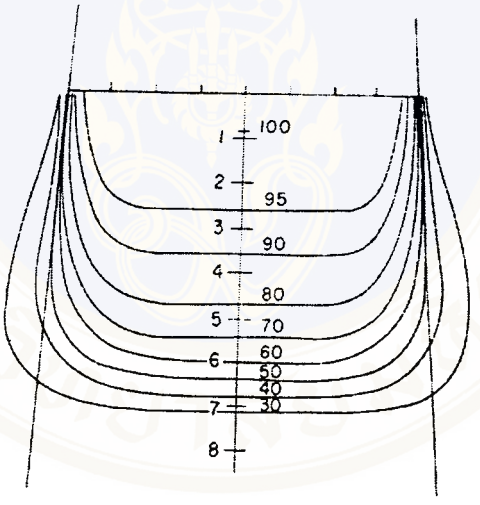

Figure 6. Isodose chart of an electron beam (16).

1.3.2.3 Field flatness and symmetry

The ICRU (17) specifies the flatness of an electron beam in terms of uniformity index in the plane perpendicular to the beam axis at the depth of half of the therapeutic range. This index is defined as the ratio of the area inside the 90% isodose line to the area inside the 50% isodose line when the normalization is made to 100%

at the beam axis in this plane. The acceptable value of the index is larger than 0.70 for field sizes larger than 100 cm^2. A peak value in the beam must be less than 103% and covering an area of less than 2 cm in diameter to avoid hot spots.

Beam symmetry is the term that compares a dose profile on one side of the central axis to that on the other. It is recommended by AAPM (18) that the cross beam profile in the reference plane should not be different more than 2% at any pair of points located symmetrically on opposite sides of the central axis.

1.4 The IORT treatment facility

1.4.1 Treatment machine and operating room

Both orthovoltage x-ray unit and electron beam from a linear accelerator can be used in IORT (2), but the later one with the energy of 6 MeV to 22 MeV is the most common (3-5). The IORT treatment unit used in this study is a linear accelerator, Varian Clinac 2100C of Ramathibodi Hospital. It is capable of generating 6 and 10 MV photon beams and 6, 9, 12, 16, and 20 MeV electron beams. Both of photon and electron beams are used for conventional external beam treatment, only the electrons are used for IORT. So, only the electron beam characteristics from a linear accelerator are proposed. If the treatment machine is a dedicated one or used for IORT treatment only, it may be installed in a treatment-operating suit with an adjoining scrub area and recovery room. The operating room needs to have proper air circulation with air conditioning, operating room light, oxygen, and vacuum. For the treatment room without operating facility, the surgery can be done in the operating room of the Surgery Department and then move the patient to the treatment room. In Ramathibodi Hospital, the operating room is next to the treatment room in the Radiology Department.

1.4.2 Applicating system

Intraoperative radiation therapy applicating systems available now are both commercial and noncommercial which can be connected to the head of an accelerator by two docking systems (19). One is hard docking which the applicator placed in the patient is attached and fixed to the head of the accelerator. This system is designed for the good reproducibility of a precise alignment and proper docking of the applicator. For the other system, soft docking (or non-docking), the IORT applicator placed in

the patients is not attached to the gantry of the therapy machine. It is fixed in the patient by clamping to the treatment couch. So between the applicator and the gantry is an air gap. The advantages of this system are safety and the ability to monitor and have the target area readily accessible at any time during treatment (20).

1.4.2.1 Hard docking IORT system

Hard docking system has two types of docking, one is side lateral docking and another one is vertical slide docking. Figure 7 shows the side lateral docking applicator system that used in Ramathibodi Hospital. It has two main components, the applicator attachment with periscopic viewer, and the IORT cone. The applicator attachment is the part that attaches the main frame adapter and the other side for docking the IORT cone. The upper portion of the applicator attachment is circular in crossection. It is slided into the fitted railing of the main frame adapter with side locking to allow proper placement of the applicator attachment. The upper part of the applicator attachment has a removable thin sheet of mylar to prevent dirt or dust falling into the surgical area. At the front of the applicator attachment has a polished stainless steel mirror that can move into the center of the applicator attachment for viewing the treatment region through the IORT cone. It is equipped with light pen for viewing the treatment area under geometrical condition. The telescope camera can be attached to the applicator attachment which allows a "beam's eye view" of the treatment area. The telescope can be separately sterilized. The lower sleeve of the applicator attachment will hold and lock the IORT cone. At the end of the sleeve has a lateral open door for IORT cone to be laterally docked into the sleeve and when the door is closed, it will keep the electron cone in proper alignment. The

applicator attachment has a knob at the side door to prevent IORT cone dropping, so the sleeve is non-adjustable length.

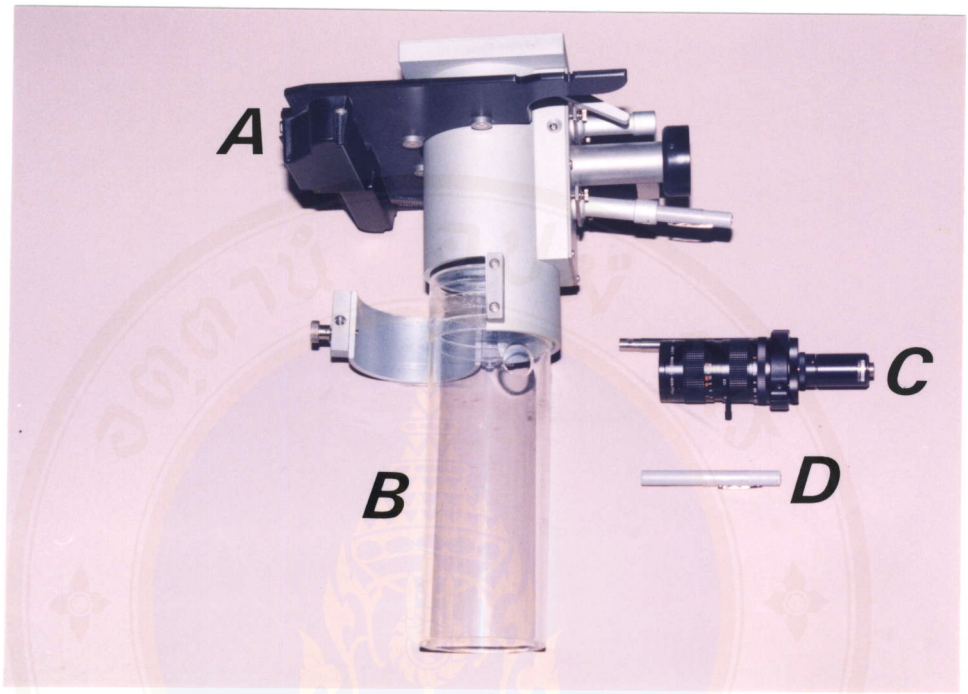

Figure 7. Hard docking IORT system (side lateral docking type), A) Applicator attachment, B) Transparent applicator, C) Telescope camera, D) Light pen.

The transparent applicator (or IORT cone) is made of acrylic in cylinder shape. It has many different diameter sizes with flat end and bevel end with various angles as shown in Figure 8. At the upper part of the acrylic has 3 acrylic spacer rings for different cone sizes to be docked in to the applicator attachment. The top of the acrylic has a thick brass plate in donut shape on each cone to collimate and prevent electron from penetrating the acrylic spacer ring (21). The brass plate has a different width equal to the spacer ring width of each cone and the width of this plate is narrower with increasing of cone diameter until no brass plate in the biggest cone diameter as shown in Figure 9.

Figure 8. Transparent applicators (flat and 30° bevel ends) of Ramathibodi Hospital.

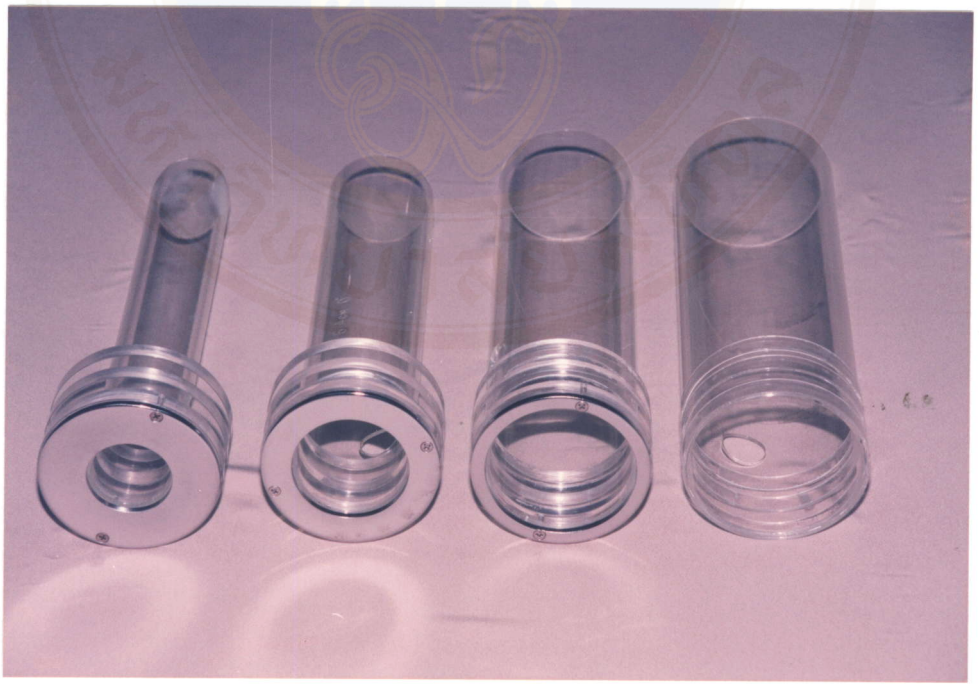

Figure 9. The different widths of the brass plates on the top of different cone diameters.

Figure 10 shows an example of the vertical slide docking type of hard dock IORT applicator system. This system has three main components, the main attachment, applicator attachment, and transparent applicator (or IORT cone). The main attachment will be attached to the main frame adapter of the treatment machine. The main attachment is made of aluminum and has a square crossection. It has a hole for inserting fiberoptic telescope which allows a "beam's eye view" of the treatment region. The telescope can be removable. It is equipped with a variable intensity light source for viewing treatment area. At the lower part has two rails for the upper portion of the applicator attachment to slide into the rails and has a pin for locking the applicator attachment in place. The upper part of the applicator attachment is a plate and lower part is a sleeve for holding and locking the IORT cone. The applicator attachment has varying sleeve size to allow the different treatment field. The transparent applicator (or IORT cone) is made of acrylic. It is slided into the sleeve and it can be locked inside the sleeve by a tension locking. The sleeve is long enough to allow for the insertion of transparent applicators to vary length for the source surface distance (SSD) adjustment at any distance in the clinical useful range. The SSD can be varied from 100 to 120 cm. This IORT cone has many different diameter sizes with flat and bevel ends.

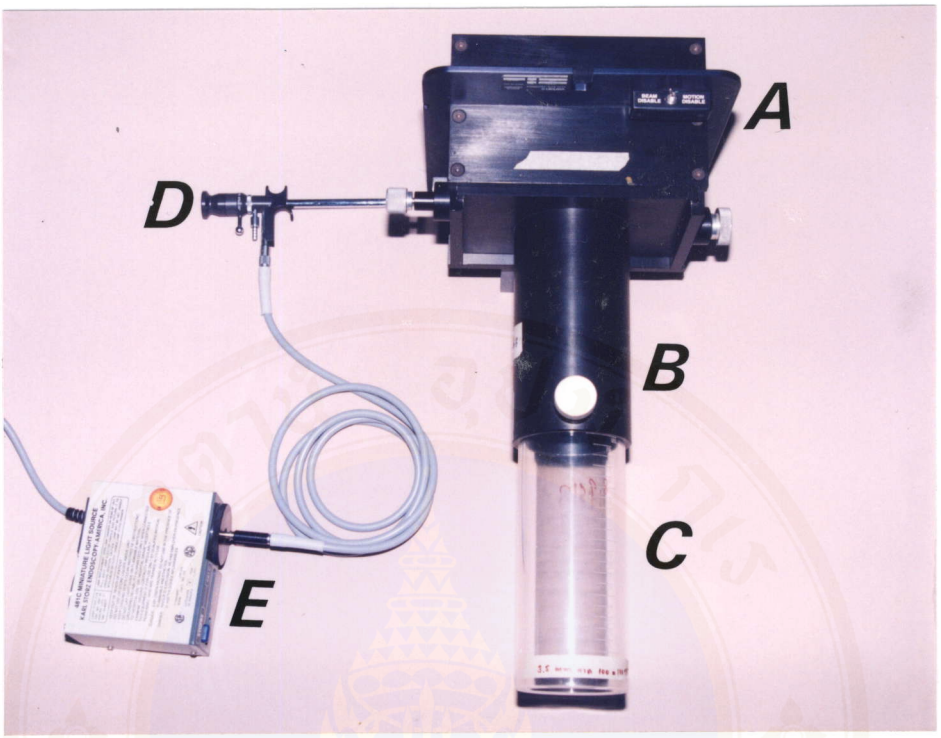

Figure 10. Hard docking IORT system (vertical slide docking type), A) Main attachment, B) Applicator attachment, C) Transparent applicator, D) Fiberoptic telescope, E) Variable light source.

1.4.2.2 Soft docking IORT system

The soft docking system consists of three main components. The first one is a cylindrical treatment cone that can be made of plastic (19) or metal (20, 22) with flat or bevel end. The second one is collimation for electron beam or primary electron applicator attached to the treatment head. The third component is a laser alignment system (23) or alignment rod (20). Since the cone is in the patient and is not attached to the primary applicator or the gantry of the machine, it needs the alignment system to align the central axis of the electron beam with the axis of the cone.

1.4.3 Dosimetric parameters (24)

Before using an IORT system in clinical treatment, a number of dosimetric parameters for each beam energy, applicator size of the machine has to be determined. For the IORT with electrons, the necessary dosimetric data are :

1.4.3.1 Central axis data :

-Depth of maximum dose (d_{max})

-Percent depth dose (%DD) or central axis depth dose

-Surface dose

-Bremsstrahlung x-ray contamination

1.4.3.2 Applicator parameters :

-Output factors

-Source-surface distance correction factors

1.4.3.3 Dose distribution data :

-Isodose curves

-Beam flatness

-Penumbra

1.4.3.4 Shielding data.

1.4.3.1 Central axis data

- The depth of maximum dose

The depth of maximum dose, d_{max}, is an essential factor in electron beam treatment. The other critical dosimetric parameters, including the output factors and %DD values, require the determination of d_{max}. The depth of d_m for each energy depends on bevel angle, SSD, applicator shape and size. It varies

minimally over the range of applicator size. Therefore a single value of d_m can be assumably used for each energy. A high surface dose and fast fall-off dose with depth are necessary in IORT treatment, since the tumor may extend to the surface of the surgically exposed tissues or the critical organ may be directly below the tumor. So dose measurement in build up region is very important

- Percent depth dose (%DD) or central axis depth dose

Accurate determination of %DD over clinically useful range is very important in electron beam therapy. Particular concern when measuring the %DD values for bevel applicators is the choice of central axis. Three geometrical configurations are possible for defining the central axis as shown in Figure 11.

A) With the first configuration as shown in Figure 11(a), the radiation beam central axis and the main tumor volume axis are congruent. This configuration will create an air gap on the central axis related to the applicator diameter and beveled angle. This air gap increases as these two parameters increase. This configuration lacks of correspondence to the actual clinical setup.

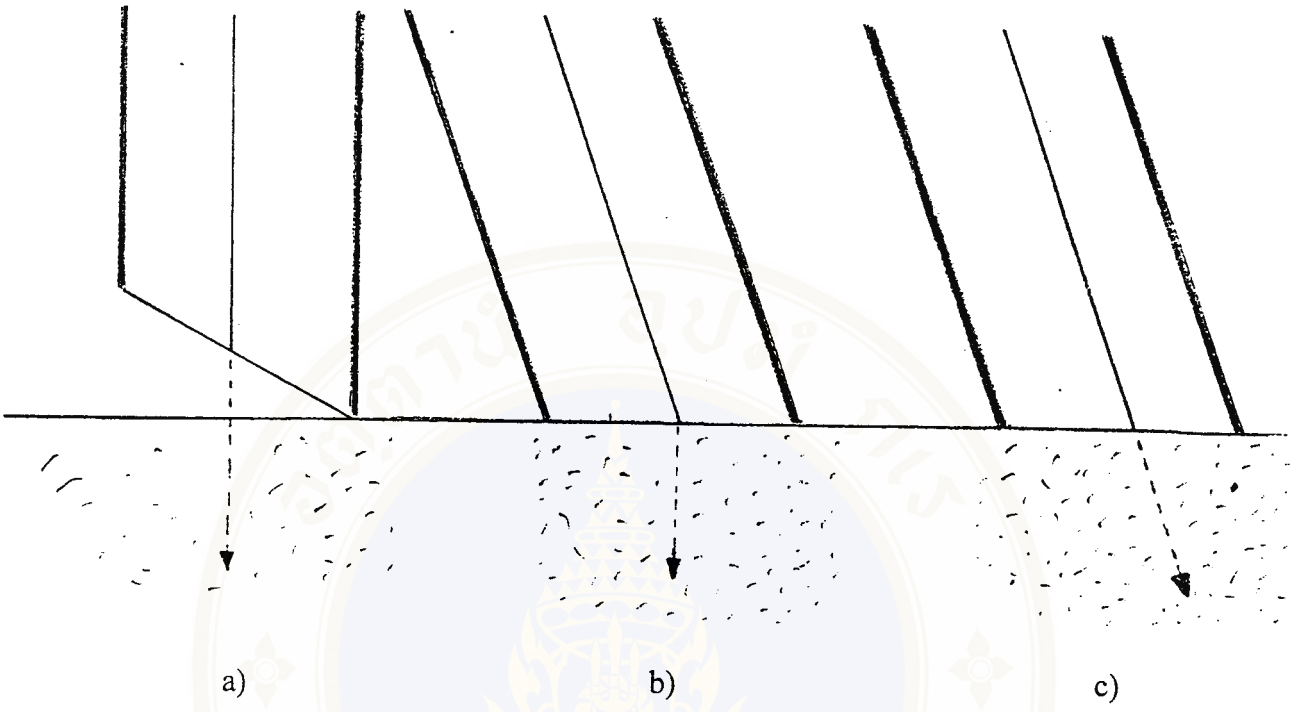

Figure 11. Three possible configurations for defining the central axis of bevel end applicator.

B) The second configuration shown in Figure 11(b) that the radiation beam data are taken along the main axis of the tumor or perpendicular to the surface. No air gap between the applicator and the phantom surface so the beam central axis does not coincide with the axis which the data are taken and the isodose distribution is not symmetric with respect to the radiation beam central axis as shown in Figure 12.

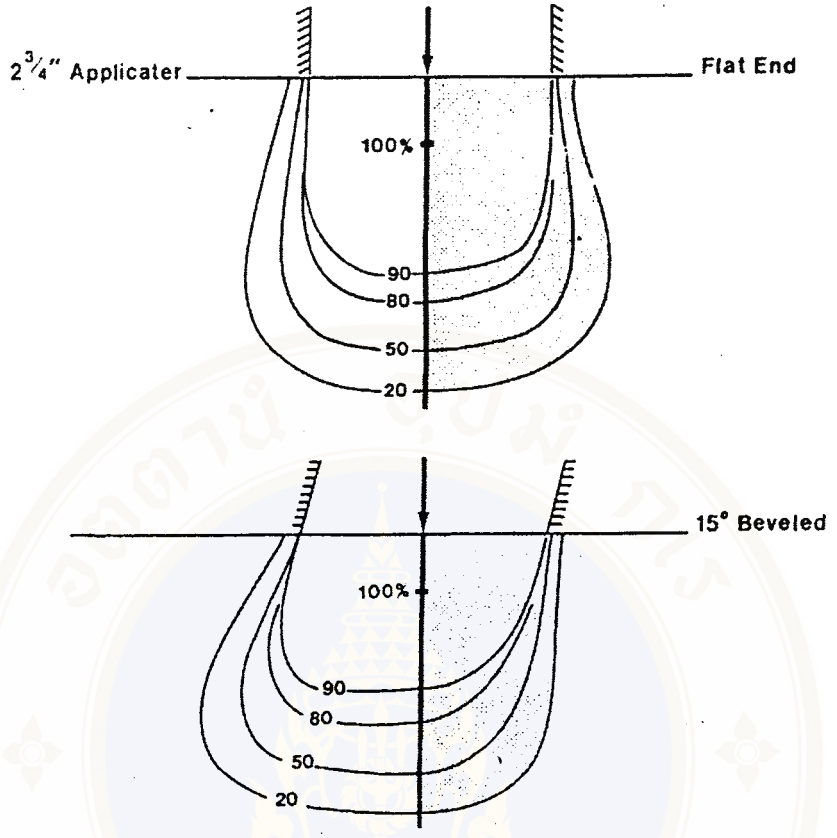

Figure 12. The dose distribution for 15 MeV electron beam of flat end and 15° bevel end applicators with the second configuration of the central axis defining (24).

Figure 13 shows the depth of penetration along the central axis that is underestimated from the actual penetration of the electron beams by a factor approximately 15%. The underestimated value depends on the SSD and bevel angle. Since the SSD is defined as the distance from the source to the bevel end on the long side of the applicator, the SSD on the central axis is reduced by a factor of 1/2 (R tan θ), where R is the diameter of the bevel applicator and θ is the bevel angle. The major advantage of this configuration is the simplicity in generating the dosimetric data in a water phantom which the detector is moved perpendicularly to the surface of the water with the gantry rotated by the appropriate bevel angle.

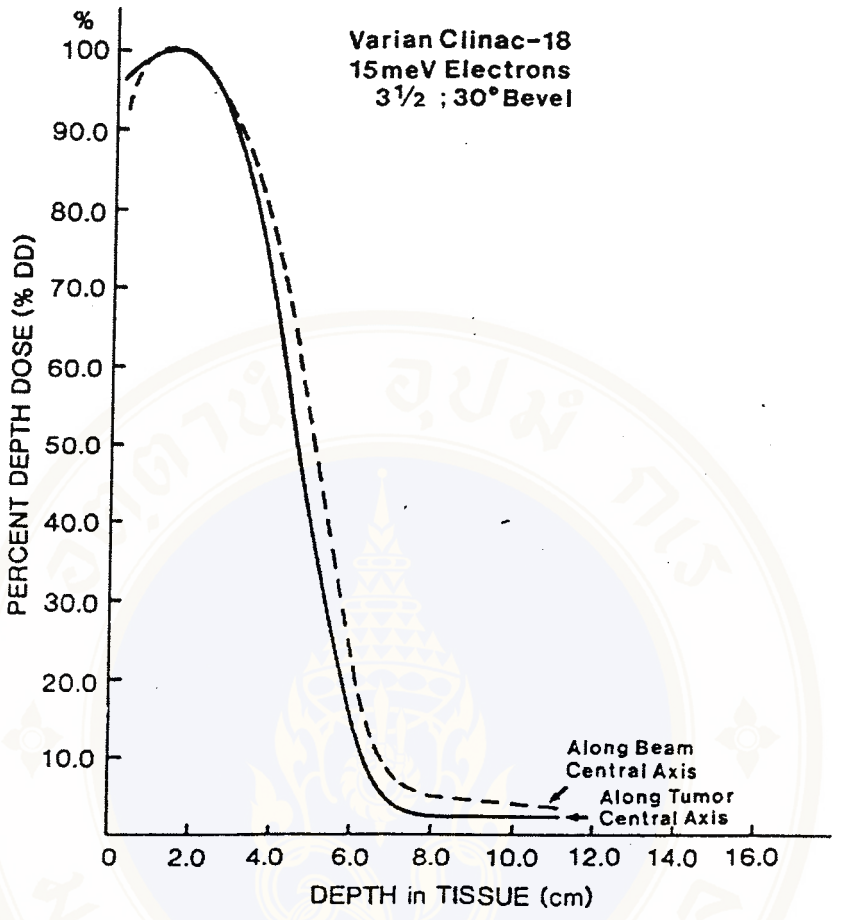

Figure 13. The %DD values along the beam axis compared with the %DD values along the tumor axis (24).

C) In the third configuration illustrated in Figure 11 (c), the bevel end of the applicator is parallel to the tumor surface and the central axis of the beam is used for dose measurements. This configuration is recommended for clinical use even through it creates difficulties in the actually dosimetry, especially when data are measured in water. The reasons of being recommended are (1) the %DD data represent the actual penetration of the radiation beam, (2) the isodose distribution is symmetric to the central axis as shown in Figure 14, and (3) the physical configuration corresponds to the treatment setup.

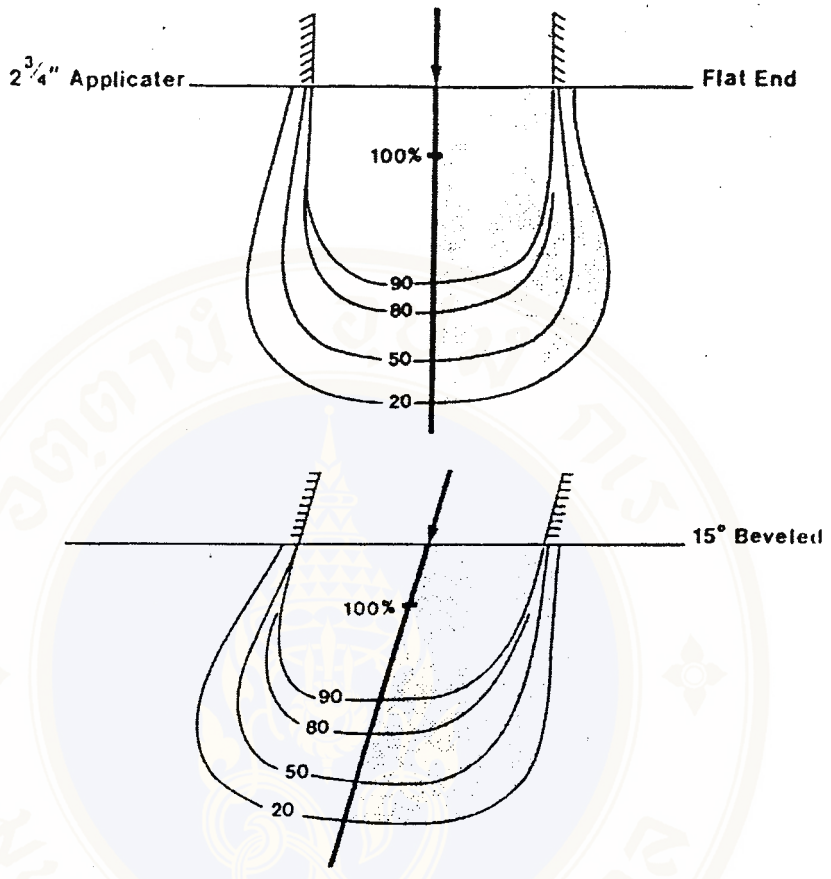

Figure 14. The dose distribution for 15 MeV electron beam of flat end and 15° bevel end applicators with the third configuration (24).

For simplicity in the generation of %DD values, it is recommended that the %DD data be measured along the main axis of the tumor (perpendicular to the phantom surface) and then the data be geometrically related to %DD on the beam axis.

- Bremsstrahlung x-ray contamination

In the case that the tumor volume is overlaid upon a critical organ, it is necessary to consider the bremsstrahlung x-ray effect beyond the electron range. The bremsstrahlung x-ray contamination is relatively constant beyond the practical range of the electrons. It contributes 2-10 % of the maximum dose (24), and its magnitude increases with increasing applicator size and beam energy. The magnitude of the bremsstrahlung x-ray contamination also depends upon the function of the primary photon collimating system. The bremsstrahlung x-ray contamination decreases with enlarging the photon jaws.

1.4.3.2 Applicator parameter

- Output factor

Output factor, the dose at d_{max} per monitor unit is one of the most important dosimetric parameters in IORT. The output factor depends upon many parameters for example photon collimator setting, electron beam energy, SSD, applicator shape, size and bevel angle.

1.4.3.3 Dose distribution data

- Isodose curves

The isodose curves for all applicators must be measured at all energies used and all for flat end and bevel end applicators because the isodose of bevel end applicator is different from the flat end applicator as shown in Figure 12 and 14.

- Beam flatness

It is necessary to measure the beam flatness of the radiation field because the radiation dose is not uniform across the IORT radiation field. This is

caused by the effect of radiation scatter from the IORT applicator wall. Figure 15 shows the horns at the side of applicator for 18 MeV electron beam. The data was taken at d_{max} along the beam central axis of the applicator. The value of the beam nonuniformity across field is 18%.

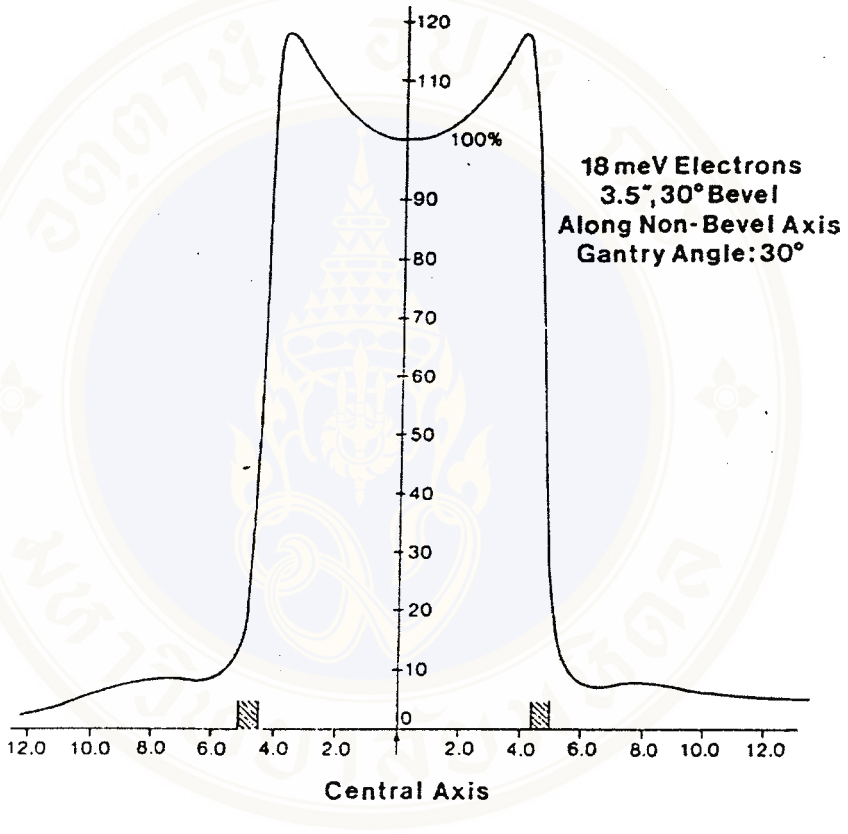

Figure 15. Beam profile of 18 MeV electron beam for 3.5 inches with 30° bevel end applicator (24).

The effect of radiation scatter on beam uniformity also depends on electron beam energy. The beam nonuniformity increases as electron energy is increased as shown in Figure 16. In IORT, field width is usually defined at the 90% isodose line in the reference plane.

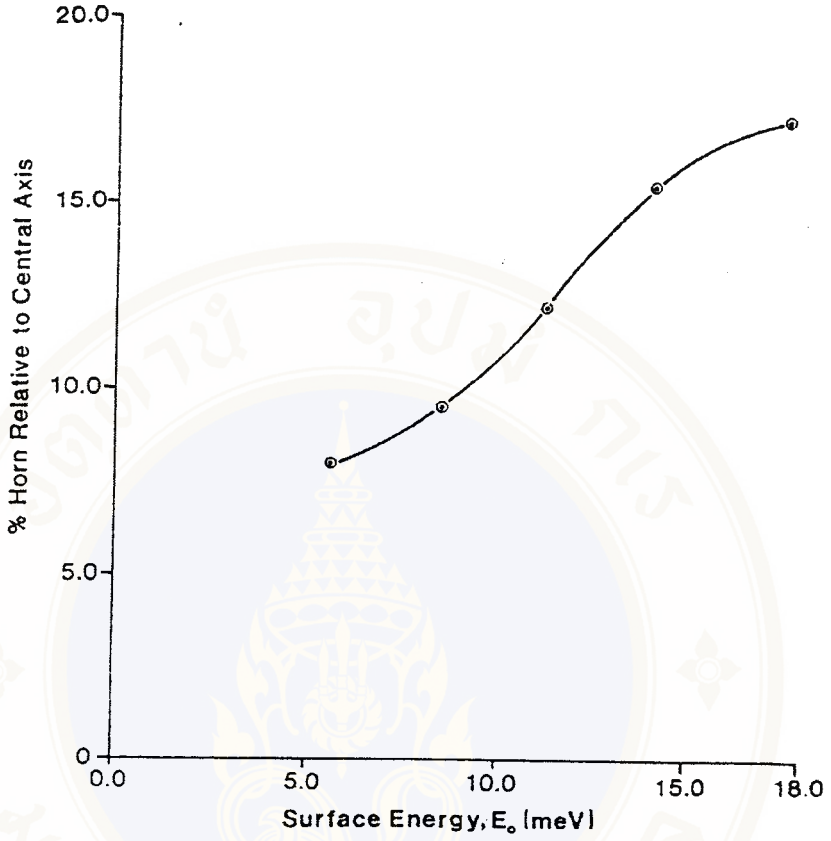

Figure 16. Percent horn relative to dose on central axis plotted as a function of energy at the surface (E_0) for 3.5 inches flat end applicator (24).

- Penumbra

Penumbra is the undesired dose outside the radiation field. It is defined at average distance separating the 80% and 20% isodose lines. The magnitude of penumbra depends on photon collimator setting and the beam energy. It can be caused by the scatter radiation from the interaction inside the radiation field and the radiation leakage through the sleeve and baseplate of the applicator attachment. In bevel end applicator, the penumbra at the short side of applicator is much higher than the long side as shown in Figure 17. The difference in penumbra value between short

side and long side of applicator increases with increasing energy because with the higher energy, the higher number of unattenuated and unscattered radiation reach the measuring point. So, in bevel end applicator, the penumbra is an important factor.

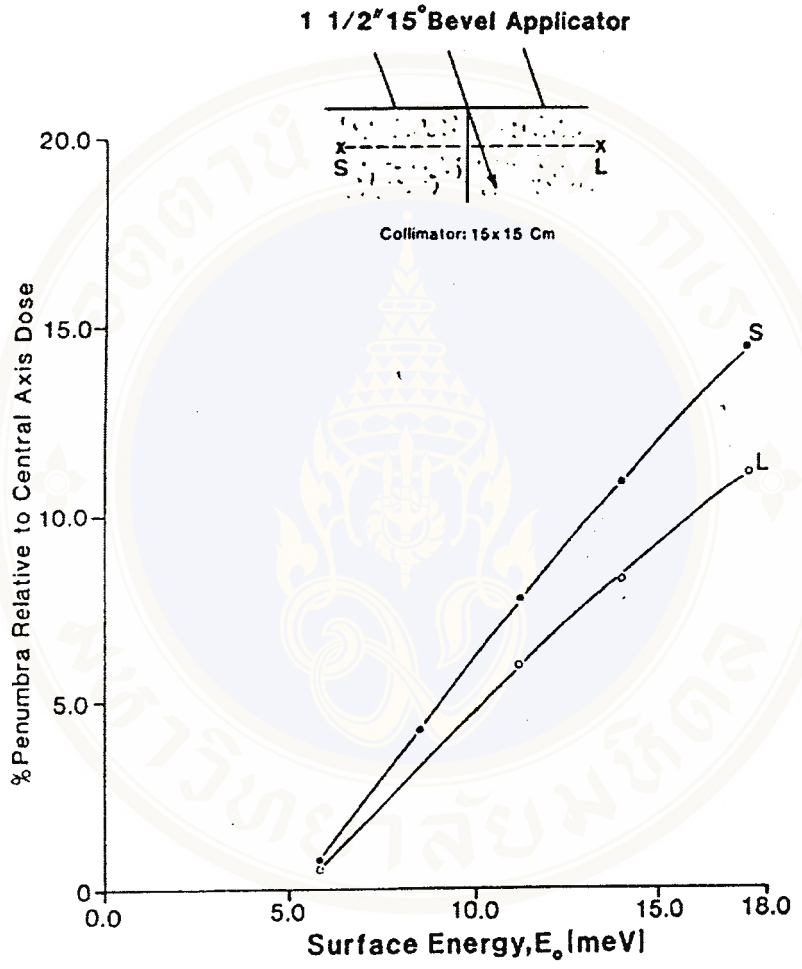

Figure 17. Percent penumbra outside the useful beam of 15° bevel angle applicator plotted as a function of electron beam surface energy (S and L refer to the percent penumbra along the short and long sides of the applicator respectively) (24).

1.4.3.4 Shielding data

The shielding data required in IORT are the thickness or number of shielding sheets for radiation transmission of 10%, 7%, 5%, and 3% for each energy.

1.4.4 Radiation leakage

In IORT treatment, the radiation leakage dose outside the useful electron field is one of the important parameters. The normal tissue being around the tumor is usually adjacent to the cone wall up to few centimeters from the end of the cone. The radiation leakage dose depends on the energy of electron beam, the photon collimator setting, the applicator system, and the distance from the source.

1.4.4.1 Dependence on the energy of electron beam

The radiation leakage outside the treatment cone increases with increasing of the electron energy due to the higher number of transmitted and scattered radiations can reach the region outside the cone (25).

1.4.4.2 Effect of photon collimator setting

The increasing of photon collimator setting increases the radiation leakage of the IORT cone (24, 25, 26). A single photon collimator setting that provides the optimum dose uniformity across the electron beam is used in many centers (24, 25).

1.4.4.3 Variation with the applicating system

The radiation leakage of the IORT cone depends on the material of the applicating system and also how it is interfaced to the therapy machine (hard docking or soft docking). The radiation leakage of the brass cone is less than the acrylic cone eventhrough the wall thickness of the later one is thicker (22).

1.4.4.4 Dependence on the distance from the source

The radiation leakage is decreased with increasing the distance from the source (25).

1.5 Thermoluminescent dosimetry (TLD)

Thermoluminescent dosimeter (TLD) is the most widely used of solid state dosimeter systems for the measurement of absorbed dose. Crystalline Materials are used as the dosimeters for this system. The radiation dose is determined by measuring the light emitted from applying of heat to the irradiated crystalline materials. The emission of light by the application of heat is called thermoluminescence (TL). The light emitted is proportional to the amount of radiation. The TLD material may be in a number of different forms such as a chip, a small cylindrical rod, and powder. Most crystalline materials exhibit the phenomenon of thermoluminescence (TL). When the materials are irradiated by ionizing radiation, they store some of the absorbed energy in the crystal lattice. Some of the stored energy is released as light after being heated. The light emitted can be measured by a photomultiplier tube (PMT). The PMT converts the light into an electrical current that is applied and measured by a recorder or meter as shown in Figure 18. The total amount of light emitted is proportional to the amount of energy absorbed from the radiation. Several TL phosphors are used for radiation measurements such as Lithium Fluoride (LiF), Lithium Borate ($Li_2B_4O_7$), and Calcium Fluoride (CaF_2), but LiF is most extensively studied and most frequently used for clinical dosimetry. The effective atomic number of LiF is 8.2 that is very close to the value of 7.4 for soft tissue and 7.68 for air (27). This makes this material be very suitable for clinical dosimetry. Lithium Fluoride is available in various forms with three relative proportions of ^6Li and ^7Li. These are 7.5% and 92.5% respectively for TLD100, 95.6% and 4.4% for TLD600, and 0.01% and 99.99% for TLD700 (28). Since the capture crossection of ^6Li for thermal neutron is large but it is small for ^7Li,

TLD600 is suitable for thermal neutron measurement while TLD100 and TLD700 are primarily used for photon measurement (28).

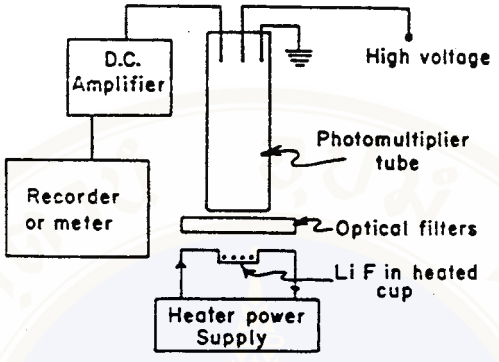

Figure 18. Diagram showing apparatus for measuring light output from thermoluminescent material (29).

The thermoluminescent dosimeter must be suitably annealed to remove residual effects of the radiation and heat every time before using and must be calibrated before being used to measure an unknown dose.

1.5.1 Annealing

The TLD has to be annealed before reusing it to move the residual effect of the previous radiation history that can effect the response of the TLD. The standard preirradiation annealing procedure for LiF is 1 hour of heating at 400 °C. For postirradiation annealing, the exposed TLD is heated at 100 °C for 10 minutes to eliminate peak 1 and 2 of the glow curve that makes the curve become more stable and predictable (28).

When an irradiated TLD is heated at a constant rate, the light emitted as a function of time follows the pattern called glow curve as shown in Figure 19.

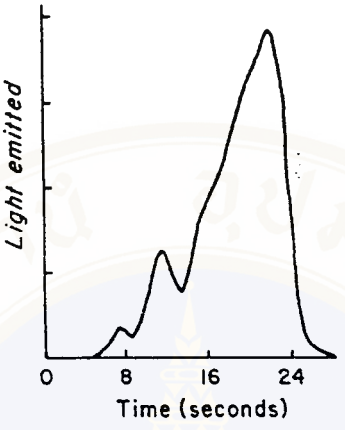

Figure 19. Glow curve for a thermoluminescent material showing relative light output as a function of heating time (29).

1.5.2 Calibration of TLD and TLD instrument

The purpose of calibrating a TLD instrument is to produce consistent and accurate reading in dosimetrically meaningful units. The calibration process involves the following 3 steps.

a) Generate calibration dosimeters

In this process, an Element Correction Coefficient (ECC) is generated by using a set of dosimeters, typically 1-2% of the total population to be calibration dosimeters. They are identified and segregated from the field dosimeters.

All dosimeters are annealed to clear them all residual exposure. Duration time between annealing and exposing should be the same for all dosimeters. After being exposed to the known radiation dose, The charge integral value (Q_i) in nC of each dosimeter (i) is read out and recorded. Then the average charge integral ($\bar{Q}$) of

all dosimeters is calculated and the Element Correction coefficient (ECC_i) for individual dosimeter i (i =1, 2, 3, ..., n) is computed by dividing the average charge integral by the individual charge (Q_i) as :

$$ECC_i = \bar{Q}/Q_i \qquad (1)$$

b) Calibration of TLD reader

A group of dosimeter about 1-2 % of dosimeters in (a) which have ECCi values close to 1 are chosen to be calibration dosimeters. The calibration dosimeters are exposed to a known amount of radiation dose (D) in grays and read by TLD reader. As Q_i is the reading for the dosimeter i, the corrected charge integral (Q_{ci}) of that dosimeter is calculated by :

$$Q_{ci} = Q_i * ECC_i \qquad (2)$$

Then the reader calibration factor (RCF) is calculated from the equation,

$$RCF = \bar{Q}_c/D \qquad (3)$$

When $\bar{Q}_c$ is the average corrected charge integral and calculated by :

$$\bar{Q}_c = 1/n \left(\sum_{i=1}^{n} Q_{ci} \right) \qquad (4)$$

c) Calibration of dosimeters

The rest of the dosimeter [number of the dosimeters in (a) - number of the dosimeters in (b)] are used as field dosimeters. They are exposed by the known radiation dose of L grays and read by TLD reader. The calibration value of ECC for individual dosimeter (ECC_{ci}) is then calculated by :

$$\mathbf{ECC_{ci} = (RFC*L)/Q_i} \qquad (5)$$

1.5.3 Determination of unknown radiation dose

The field dosimeters in 1.5.2 (c) are used to measure unknown radiation dose. The unknown dose D in grays is calculated by using ECC_{ci} from the equation (5) :

$$\mathbf{D = (Q_i*ECC_{ci}) / RCF} \qquad (6)$$

When Q_i is the reading of the individual field dosimeter i.

1.6 Film dosimeter

A radiographic film consists of very small crystals of silver bromide embedded in an emulsion on a transparent film base (cellulose acetate or polystyrene resin) (30). If the film is exposed to an ionizing radiation or visible light, a latent image is formed by a chemical changing process within the exposed crystals. When the film is developed, the crystals altered by the radiation are reduced to small grains of metallic silver. The film is then fixed to dissolve the unaffected bromide, leaving a clear film in its place. The metallic silver, which is not dissolved by the fixer, causes darkening of the film. The blackening of the film depends on the amount of the metallic silver deposited and, consequently, on the radiation energy absorbed. This relationship exists as long as the amount of uneffected grains is large in comparison to the number of affected ones. If the film is exposed to a large dose, more of the grains already hit by the radiation are hit again.

A densitometer is used to measure the concentration of metallic silver grain (the degree of blackening of the film) by determining the optical density (OD). This instrument has a light source, a tiny aperture and a light detector (photocell) to measure the light intensity transmitted through the film. The optical density may reach a limit if the film is exposed to a large exposure and then decreases with increasing exposure as shown in Figure 20.

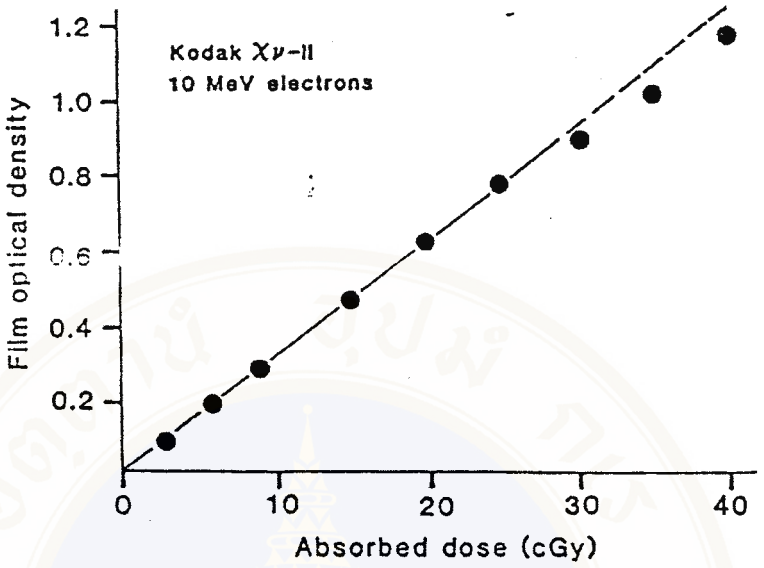

Figure 20. The characteristic curve (optical density-dose response curve) of a film exposed to a 10 MeV electron beam (31).

The densitometer gives a direct reading of optical density if it has been calibrated by a standard strip of film which have the region of known optical density. In dosimetry, the net optical density is obtained by subtracting the reading from the base of fog (OD of unexposed processed film). Densitometers used in photographic dosimeter are usually capable of measuring OD values from 0 to 4 (32).

The response of a film to radiation with different energy will be influenced by the emulsion thickness and the ratio of silver halide to gelatin in the emulsion and also the development conditions. For relative measurements on a single sheet of film, the variations from film to film or of development conditions, are minimized.

CHAPTER II

OBJECTIVES

In an intraoperative radiation treatment (IORT), the normal tissues are usually extend along the outer wall of the treatment cone up to about 4 cm from the cone end. A large single dose is delivered to the tumor, so the radiation leakage outside the treatment cone is very important. This study was designed to determine the leakage radiation outside the treatment cone wall of the IORT applicating system attached with the linear accelerator of Ramathibodi Hospital. The aims of this investigation are as the followings :

1 Determination of the maximum leakage radiation at the outer wall of the IORT cone for the distance of 0-8 cm from the end of the treatment cone.

2 Comparison of the maximum leakage dose of the cone sizes with 4.5, 6.4, 8.3, and 9.5 cm diameters for 6, 12, and 20 MeV electron beams.

3 Determination of the maximum radiation dose to the normal tissues surrounding the outer wall of the cones.

CHAPTER III

LITERATURE REVIEW

Bagne et.al. (25) determined the radiation contamination outside the applicator by measuring the beam profile in water phantom at the depth of maximum dose by using Therados Radiation Field Analyzer with the associated with a microchamber and a diode detector. They reported that the magnitude of the radiation contamination increased with increasing electron beam energy, collimator size. For 15x15 cm collimator setting with acrylic cone of 1/2 inch thickness for 18 MeV electron beam, the highest radiation leakage and contamination was 18% of the central axis dose.

Hogstrom et.al. (22) measured the electron leakage through the walls of 1 mm thick brass cone and 5 mm thick acrylic cone (non-docking) with 7 cm diameter for 18 MeV by using radiographic films and solid water phantom. The films were exposed in the plane perpendicular and also parallel to the central axis. They reported that the electron leakage was greatest at the upper portion of the cone where the electrons have the greatest angle of incidence. The maximum leakage was 8% of the central axis maximum dose for the brass cone and 16% for the acrylic cone.

Palta and Suntharlingam (33) measured the leakage through a 10 cm diameter lucite cone with 6.35 mm wall thickness (non-docking IORT cone system) in air and water by using the scanning system with two shonka plastic 0.147 cm^3 volume ionization chambers. They showed the doses at various distances from the top of the

cone relative to the maximum dose in water on the central axis of cone at 100 cm SSD. The radiation leakage around the bottom half of cone for 22 MeV electron beam was less than 10%, but in the regions close to the wall at upper part of the cone was as high as 22%.

Kharrati and Guillemin (23) used plane parallel ionization chamber (Markus, M23343) and DI 4-DL 4 PTW electrometer to measure the leakage dose through 5 mm thick acrylic cone of non-docking IORT applicator system. They showed that the leakage radiation outside the cone wall with the shielding plate of 2 mm thick Pb and 1.5 mm thick Al was less than 5% for all energies between 6 MeV and 13.5 MeV.

CHAPTER IV

MATERIALS AND METHODS

4.1 Materials

4.1.1 Linear Accelerator

Clinac 2100C of Varian with five electron beam energies 6, 9, 12, 16 and 20 MeV, and two photon beam energies 6 and 10 MV was used in this experiment. The machine has standing wave guide, side coupling cavity accelerator with tungsten target, dual scattering foil to make electron beam intensity more uniform across treatment field, triode electron gun. Klystron is used to amplified RF pulse to generate the high power-microwave energy. Ion chamber is used to monitor the radiation output. Five stationary therapy dose rates range from 80-400 monitor units per minute at standard target to surface distance (TSD). Target to isocenter distance of this linear accelerator is 100 cm. Photon field sizes range from 0.5x0.5 cm to 40x40 cm at isocenter and electron applicator of 4x4, 6x6, 10x10, 15x15, 20x20, and 25x25 cm (34, 35).

4.1.2 Intraoperative electron cone system

The IORT applicating system used in the experiment is a commercial hard docking cone of Radiation Products Design, Inc. It has two main components, the applicator attachment with periscopic viewer, and the IORT cone.

4.1.2.1 Intraoperative radiation therapy cones

Intraoperative radiation therapy cones used in Ramathibodi Hospital are made of clear acrylic cylinder which is 3.1 mm thick and 30.5 cm long as shown in Figure 8 and Figure 9. The top of the cone has three acrylic spacer rings to allow the different cones size to slide into the barrel of viewer. Donut shape of 4.8 mm thick brass plate is mounted to the top of each cone to collimate and prevent electron from penetrating the acrylic spacer rings. Each cone has a 2.5 cm diameter hole at its side to allow easy access for TLD placement or fiber optics light source.

4.1.2.2 Periscopic viewer

Periscopic viewer is the part that attached to the linear accelerator treatment head and the other side has a barrel sleeve for the IORT cone to be docked in. At the end of barrel sleeve has a lateral open door for the electron cone to be laterally docked in to the barrel. When the door is closed, it will keep the electron cone in proper alignment and then the door is closed and the IORT cone is locked to prevent cone dropping. At the side of viewer has a polished stainless steel mirror that can be moved into the center of barrel for viewing the area of treatment through the electron cone. The top of barrel has 0.002" sheet of mylar to prevent foreign matter entering into treatment area. All of the IORT cone system has different sizes with diameters 4.5, 5.7, 6.4, 7.6, 8.3, 8.9, and 9.5 cm of two types of cone end, flat and 30° beveled.

4.1.3 Automatic isodose plotter system

The automatic isodose plotter system used in the experiment is a water phantom system, RFA300 Radiation Field Analyzer of Scanditronix as illustrated in

Figure 21. The water phantom with scanning volume of 495 x 495 x 495 mm is fitted with a precision servo mechanism for full three dimensional detector positionings. It also allows positioning of the field detector to measure both vertical and horizontal beams with a window of 10 mm wide, covered with 0.1 mm mylar film. This system can perform linear scans to measure profiles, depth doses, two-dimensional dose distribution, isodose calculation, point integration, parameter extraction, TMR measurement and real-time isodose tracking. The system has three semiconductor detectors, one for electron, one for photon, and one for reference detector.

Both field detectors allow field measurement with high spatial resolution due to the small size of the active semiconductor chip. The chip is very close (0.5 mm) to the front of the field detector so it can be positioned near the phantom surface (36).

Figure 21. The linear accelerator with RFA300 Radiation Field Analyzer.

4.1.4 Thermoluminescent dosimeter (TLD) system

The thermoluminescent dosimeter (TLD) used in this research is LiF700 with automatic TLD reader, model 5500 of Harshaw Bicron as shown in Figure 22 and Harshaw Bicron TLD oven for annealing the thermoluminescent dosimeter.

4.1.4.1 Thermoluminescent dosimeter oven

Harshaw Bicron TLD oven used in annealing the thermoluminescent dosimeters is operated by two programs (37), program 1 for annealing TLD before irradiation and program 2 for preheat after irradiation before reading by TLD reader. Program 1 is heating to 400 °C, keeping temperature for 60 minutes. Then cooling to 100 °C, keeping temperature for 120 minutes, and cooling to 45 °C (end of program 1). Program 2 is heating to 100 °C, keeping temperature for 10 minutes. Then cooling to 45 °C(end of program 2) (37).

A fan is used to circulate the hot air for equal temperature distribution through the oven. This oven can be used to anneal chip, ribbon and rod types of TLD by placing them on aluminum or stainless steel tray which fits in the oven.

4.1.4.2 Thermoluminescent dosimeter reader

The Harshaw model 5500 automatic TL reader used in this study is a PC-driven, table-top instrument for TLD measurement. In one loading, it can read 50 dosimeters within variety features of TLD, for example chips, rods and cubes also with TLD100 and TLD700 too. The reader can be configured to calibrate the instrument in grays, sieverts and the other calibration units.

Hot nitrogen gas heating with a closed loop feedback system used in the reader produces linearly ramped temperatures with the accuracy of ± 1°C to 400 °C.

To maintain consistent performance of the PMT, the photomultiplier tube assembly is cooled to a constant temperature. Nitrogen is routed through the PMT chamber to eliminate condensation. Measurement range of this equipment is 10 μGy (1 mrad) to 10 Gy: linear and 1 Gy (100 rad) to 20 Gy (2,000 rad): supralinear (38). This equipment has fading correction algorithm and glow curve batch deconvolution. Its repeatability is less than 2% variation and the residual TL signal less than 2% variation based on one standard deviation for ten sequential measurement at 1 mGy of Cs-137. Its minimum detectable is less than 10 μGy (1 mrad).

Figure 22. The automatic thermoluminescent dosimeter reader.

4.1.4.3 Thermoluminescent dosimeter

Commercial TLD 700 (LiF) rods of Harshaw Chemical were used in this experiment. It's physical properties is rod form, size 1 x 1 x 6 mm^3. Lithium Fluoride is an alkali halide with density of 2.64 g/cm^3 and atomic number (Z_{eff}) = 8.2,

nearly to air (7.68) and soft tissue (7.4). It is composed of ^{6}Li 0.01 %, ^{7}Li 99.99 % (28). This TLD material is produced by homogeneous melting of lithium fluoride, magnesium fluoride, lithium cryolite and lithium titanium fluoride, resulting in a phosphor containing 300 ppm magnesium and 10-20 ppm titanium.

4.1.5 Film dosimeter

Non screen, high speed film (Kodak X-Omat TL) ready pack was used for the radiation leakage measurement around the IORT cones. It is direct exposed. For the development process, Kodak X-Omat 270 RA processor was used. The density of the film was read by using X-Rite301 black and white transmission densitometer (Figure 23) which has three sizes of apertures. The range of optical density is 0-4.0 with 1 mm aperture and 0-5.0 with 2 and 3 mm apertures.

Figure 23. Film densitometer.

4.1.6 Solid water phantom

The commercial solid water phantom of Radiation Measurement Inc (RMI) was used in determination of maximum leakage area by using films. It is composed of epoxy rasins and powders with square size of 30x30 cm^2, and thickness 0.2-5.0 cm. Its physical properties are 1.00 g/cm^3 of mass density and the number of electrons per gram of $3.34x10^{23}$. It can be used to calibrate both electron and photon beams in radiotherapy (39).

4.2 Methods

The leakage radiation outside the IORT cones for 6, 12 and 20 MeV electron beams from The Clinac 2100C linear accelerator of Ramathibodi Hospital was determined. The leakage measurements were made for the cone sizes 4.5, 6.4, 8.3 and 9.5 cm diameters both flat end and 30° beveled end. The single x-ray collimator setting of 12x12 cm was used for all cone sizes and energies.

4.2.1 Maximum leakage determination

Kodak ready pack films (X-Omat-TL) from the same pack were used to search for the maximum radiation leakage area at the outer wall of the IORT cones. Before wrapping the film around the cone as shown in Figure 24, some holes were punched near the corner of the film envelope to remove air pockets between the film surface and the envelope. For each cone size and energy, the film was irradiated by the appropriate monitor units for the film optical density about 1-3. After being developed by the Kodak X-Omat 270RA processor with the same temperature of 34.2 °C. The optical density (OD) of the films were read at every 1 cm^2 around the cone wall by using X-Rite301 film densitometer. Only the density of the film related to the lower part of the cone with 8 cm from the cone end was read. Since during the IORT, the normal tissues will not extend higher than 8 cm.

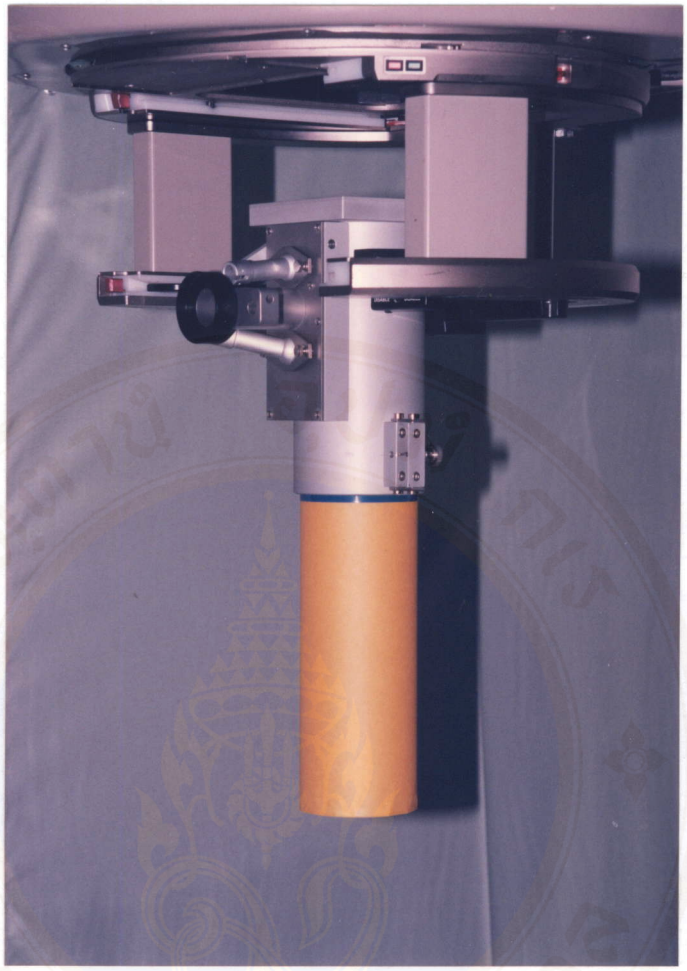

Figure 24. The irradiation technique in the determination of the maximum leakage outside an IORT cone by using a radiographic film.

4.2.2 Determination of the depth of maximum dose

The scanning system of scanditronix (RFA300) was used to determine the depth of maximum dose (d_{max}) along the central axis in the water phantom. The depths of maximum dose along the central axis of IORT cone diameters 4.5, 6.4, 8.3 and 9.5 cm with both flat and 30° bevel ends, and all for the energies of 6, 12 and 20 MeV were searched. The configuration shown in Figure 11 c was used to define the

central axis of the bevel end cones. Two semiconductor detectors were used with the scanning system, one as and electron field detector and another one as a reference detector.

4.2.3 Calibration of the output of a cobalt-60 machine

The γ-ray beam from a cobalt-60 teletherapy machine, Theratron 780C of AECL (Atomic Energy of Canada Limited) was used to calibrate thermoluminescent dosimeters. The output in air of the machine was measured by using a Capintec dosimeter with 0.6 cc Farmer type ionization chamber at 80 cm SAD (Source to axis Distance) for $10x10cm^2$ field size. Five readings were averaged and corrected for timing error, the temperature and pressure to be the exposure rate in air (X°). The absorbed dose rate in a small mass of tissue in air (D_a^0) was calculated by the following equation (40) :

$$D_a^0 = X°.f_{med}.A_{eq} \qquad (7)$$

where f_{med} = roentgen to cGy conversion factor for tissue = 0.963 cGy/R,

A_{eq} = the transmission factor representing the ratio of the energy fluence at the center of the equilibrium mass of tissue to that in free air at the same point that is 0.985 for the γ-rays from a cobalt-60 machine.

The absorbed dose rate (D_d^0) at depth d in phantom was determined by the equation (8) :

$$D_d^0 = D_a^0 TAR_{(d,s)} \qquad (8)$$

where $TAR_{(d,s)}$ = tissue air ratio at depth d for side of equivalent square field of s cm.

The irradiation time for radiation dose (TD) at the depth of maximum dose (0.5 cm) used to calibrate thermoluminescent dosimeter was calculated by the equation :

$$\text{Time} = TD/D_d^0 \qquad (9)$$

4.2.4 Calibration of thermoluminescent dosimeter

Before being used to measure the leakage radiation, the thermoluminescent dosimeters (LiF700) were calibrated in solid phantom with gamma rays from Theratron 780C cobalt-60 teletherapy machine by the following process :

a) All TLDs (77 TLDs) were annealed at 400 °C for 1 hour and 100 °C for 2 hours to clear the remaining exposure in the TLDs.

b) The TLDs were irradiated in the perspex phantom by a gamma ray beam from the cobalt-60 machine with the exposure time for 0.2 Gy as calculated in equation (9). Then they were pre-read annealed at 100 °C for 10 minutes before being read in nanocoulombs (nC) by TLD reader.

c) The Element Correction Coefficient (ECC_i) for each TLD was calculated by using equation (1).

d) From the ECC_i in (c), six of TLDs that had the ECCi values close to 1 were chosen to be calibration dosimeters.

e) Calibration dosimeters in (d) were irradiated by 0.2 Gy of gamma rays from the cobalt-60 machine and read by the TLD reader with the same technique in

(b). By using equation (3), the RCF (reader calibration factor) value of the reader was calculated.

f) The rest of TLDs (57 TLDs) from (d) or field dosimeters were calibrated by being annealed and then exposed by the dose 0.2 Gy of gamma rays from the cobalt-60 machine. After reading, the calibration value of each TLD or ECC_{ci} was determined by equation (5).

4.2.5 Measurement of leakage radiation by using the TLDs

The leakage doses were measured by using the field TLDs calibrated in the section 4.2.4(f) that had calibration factors already. The measurements were made at the points with maximum density for each distance of 0, 2, 4, 6, and 8 cm from the cone end as remarked by stars (*) in Table I-VIII. Two TLDs were strapped at each measured point on the outer surface of the cone wall (parallel to the central axis of the beam). The tissue equivalent material, superflab with 2 cm thick represented a normal tissue was wrapped around the cone as shown in Figure 25. The dose measurement at d_{max} was also made for every cone and energy by placing three TLDs on the solid water phantom and put the superflab with the thickness of d_{max} on the top of them (Figure 25).

The gantry of the linear accelerator was set at 0 degree and 30 degrees for flat end and bevel end cones respectively. The irradiation time for the absorbed dose of 0.2 Gy at d_{max} was used for each measurement. All IORT applicator set was hard docking and the secondary collimators were set at 12x12 cm for all cone sizes and energies.

The reading (Q_i) in nC for each TLD was converted to absorbed dose in Gy by equation (6). The measurements were repeated three times for each cone and energy.

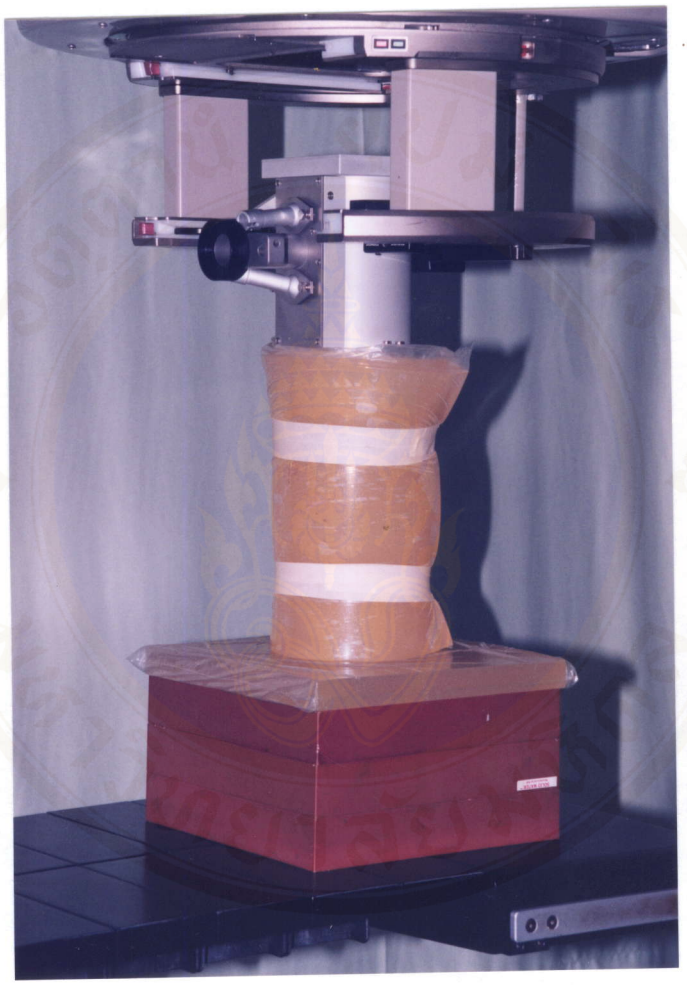

Figure 25. The irradiation technique for leakage measurements by using thermoluminescent dosimeters (TLDs).

4.2.6 Calculation of the radiation leakage dose.

The leakage doses in grays for each cone and energy from three measurements in section 4.2.5 were averaged and then normalized by the dose at d_{max}.

4.2.7 Precision test for the dose measurements by using the TLDs.

After being used in the leakage measurements, a precision test for all TLDs was performed. They were irradiated by a known radiation dose of 0.2 Gy from the cobalt-60 machine and then read by the TLD reader.

CHAPTER V

RESULTS

5.1 The maximum radiation leakage

Table I-VIII show the radiation leakage as the optical density around the wall of the cone diameter 4.5, 6.4, 8.3, and 9.5 cm (flat and beveled ends), and all for 6, 12, and 20 MeV. The radiation leakage increased with increasing of the distance from the cone end for every cone size and energy. These results are consistent with the measurement of 10 cm diameter cone for 22 MeV by Palta et al (32).

5.2 The depths of maximum dose

As shown in Table IX, the depth of maximum dose in water phantom for 6 MeV was much less than the value of 12 and 20 MeV for every cone size. For 6 MeV, the depth of maximum dose was the same for every cone size but it increased with cone size for 12 and 20 MeV.

5.3 Calibration of TLD

The Element Correction Coefficient (ECC_{ci}) values of 57 TLDs varied from 0.982 to 1.019 with the mean value of 1.00 and SD value of 0.016. The variations were within the acceptable range (38). The Reader Calibration Factor (RCF) values were 140.423 nC/Gy. The precision test of all filed TLDs by exposing the known radiation dose of 0.20 Gy showed the mean dose of 0.202 Gy (+1.2%) with 0.71 standard deviation.

5.4 Leakage doses at the outer wall surface of the cones

Table X shows the leakage doses as the percentage of the maximum dose in the central axis measured by the TLDs for 4.5, 6.4, 8.3, and 9.5 cm, cone sizes both flat and bevel ends at 6, 12 and 20 MeV. The result measured by TLDs agrees with the one by films which the radiation leakage was higher at the area closer to the source (the top of the cone). Figure 26-29 are the plots of the percent leakage doses (maximum value for each distance) relative to the dose at d_{max} from table X as a function of distance from the cone end. They show that the percent leakage doses increased linearly with the distance from the end to the top of the cone. The increasing was more rapidly for the higher energies. For up to the distance of 8 cm from the cone end, the maximum percentage of the leakage was 23.10% at 8.3 cm diameter cone with bevel end of 20 MeV. Every cone with bevel end showed higher leakage dose than the flat one for the same energy with the maximum value of 3.95% of the tumor dose for 4.5 cm cone of 20 MeV. The leakage dose increased with the energy and also cone size except the 8.3 cm cone which showed higher leakage than the larger cone of 9.5 cm. The reason may be that the 8.3 cm cone and all smaller cones have a brass plate at the top of the cone but the largest one (9.5 cm) does not have it (Figure 9). Therefore, the increasing of the leakage would be contributed by the bremsstrahlung and scattered electrons generated in the brass plate of 8.3 cm cone.

In IORT, the normal tissues extending along the outer wall of the treatment cone are normally not higher than 4 cm from the cone end. The percent leakage dose at 4 cm from the cone end of every cone size with each energy (from table XI) was

converted to the percentage of tumor dose at the treatment depth of 90% depth dose and shown in table XII. For the treatment depth of 90%, the normal tissue at the cone end and at 4 cm from the cone end would receive the maximum doses of 20.73% and 23.27% of the tumor dose respectively if treated by the 8.3 cm cone with bevel end for 20 MeV electron beam.

Table I. The optical density of radiographic film at various points on the cone surface starting from the cone end up to the distance of 8 cm from the cone end of the cone diameter 4.5 cm with flat end.

a) For 6 MeV.

Distance from cone end	**Collimator angle related to the point on the surface of IORTcone**															
	0°	26°	52°	78°	90°	104°	130°	156°	180°	208°	234°	260°	270°	286°	308°	334°
8 cm	2.04	2.04	2.02	2.02	2.02	2.02	2.03	2.00	1.95	1.95	**2.08***	**2.07***	2.07	2.07	2.06	2.06
7 cm	2.03	2.03	1.99	2.00	1.99	2.00	2.01	1.98	1.93	1.93	2.05	2.05	2.05	2.05	2.05	2.05
6 cm	2.02	2.01	1.98	1.98	1.98	1.98	1.98	1.96	1.90	1.90	**2.03***	**2.03***	2.03	2.03	2.03	2.03
5 cm	2.00	1.99	1.96	1.96	1.96	1.95	1.96	1.93	1.88	1.89	2.02	2.01	2.01	2.01	2.01	2.01
4 cm	1.98	1.97	1.95	1.95	1.95	1.94	1.95	1.93	1.87	1.85	**2.00***	**2.00***	2.00	1.99	1.99	1.99
3 cm	1.96	1.96	1.95	1.94	1.94	1.93	1.94	1.91	1.85	1.84	1.97	1.97	1.98	1.97	1.97	1.97
2 cm	1.95	1.95	1.94	1.92	1.92	1.91	1.92	1.88	1.85	1.83	**1.96***	1.95	**1.96***	1.96	1.95	1.95
1 cm	1.93	1.94	1.93	1.91	1.91	1.90	1.90	1.87	1.82	1.82	1.92	1.94	1.94	1.94	1.94	1.94
0 cm	1.92	1.92	1.91	1.90	1.88	1.88	1.89	1.86	1.82	1.80	1.91	**1.92***	**1.93***	1.92	1.92	1.92
average	1.98	1.98	1.96	1.95	1.95	1.95	1.95	1.92	1.87	1.87	1.99	1.99	2.00	1.99	1.99	1.99

* The area that radiation dose measurement by TLD was made.

b) For 12 MeV.

Distance from cone end	Collimator angle related to the point on the surface of IORTcone															
	0°	26°	52°	78°	90°	104°	130°	156°	180°	208°	234°	260°	270°	286°	308°	334°
8 cm	1.25	**1.27***	**1.27***	1.26	1.24	1.21	1.17	1.15	1.13	1.12	1.14	1.17	1.18	1.20	1.22	1.25
7 cm	1.22	1.23	1.24	1.24	1.21	1.19	1.15	1.13	1.10	1.10	1.11	1.14	1.16	1.17	1.20	1.22
6 cm	1.19	**1.21***	**1.22***	1.21	1.20	1.17	1.13	1.11	1.09	1.09	1.10	1.11	1.14	1.15	1.17	1.19
5 cm	1.17	1.20	1.21	1.19	1.18	1.15	1.12	1.10	1.07	1.07	1.08	1.10	1.12	1.13	1.15	1.17
4 cm	1.16	**1.17***	**1.18***	1.17	1.16	1.13	1.10	1.06	1.05	1.05	1.06	1.08	1.10	1.11	1.13	1.15
3 cm	1.14	1.16	1.16	1.15	1.16	1.12	1.07	1.03	1.04	1.04	1.03	106	1.10	1.10	1.11	1.13
2 cm	1.12	**1.15***	**1.15***	1.13	1.13	1.11	1.09	1.02	1.03	1.01	1.00	1.04	1.08	1.09	1.09	1.12
1 cm	1.13	1.14	1.18	1.16	1.15	1.12	1.09	1.02	1.03	1.01	1.02	1.05	1.09	1.09	1.10	1.13
0 cm	1.17	**1.21***	**1.23***	1.21	1.19	1.16	1.17	1.10	1.18	1.09	1.12	1.13	1.20	1.21	1.10	1.13
average	1.17	1.19	1.20	1.19	1.18	1.15	1.12	1.08	1.08	1.06	1.07	1.10	1.13	1.14	1.14	1.17

* The area that radiation dose measurement by TLD was made.

c) For 20 MeV.

Distane from cone end	Collimator angle related to the point on the surface of IORTcone															
	0°	26°	52°	78°	90°	104°	130°	156°	180°	208°	234°	260°	270°	286°	308°	334°
8 cm	**1.29***	**1.27***	1.26	1.24	1.21	1.19	1.15	1.17	1.24	1.21	1.20	1.15	1.13	1.13	1.14	1.15
7 cm	1.26	1.24	1.23	1.21	1.17	1.16	1.12	1.14	1.21	1.19	1.16	1.13	1.10	1.10	1.11	1.12
6 cm	**1.22***	**1.21***	1.10	1.18	1.15	1.14	1.13	1.11	1.20	1.17	1.13	1.10	1.08	1.08	1.09	1.09
5 cm	1.20	1.19	1.18	1.15	1.13	1.11	1.11	1.09	1.17	1.14	1.10	1.08	1.06	1.06	1.07	1.07
4 cm	**1.18***	**1.16***	1.15	1.13	1.09	1.09	1.08	1.10	1.14	1.12	1.09	1.05	1.03	1.04	1.04	1.05
3 cm	1.15	1.14	1.12	1.10	1.08	1.09	1.06	1.04	1.11	1.08	1.07	1.03	1.01	1.02	1.03	1.03
2 cm	**1.14***	**1.12***	1.12	1.09	1.07	1.07	1.06	1.02	1.08	1.07	1.05	1.01	1.00	1.01	1.02	1.02
1 cm	1.14	1.13	1.13	1.08	1.07	1.08	1.06	1.02	1.09	1.08	1.05	1.01	1.00	1.02	1.03	1.02
0 cm	**1.21***	**1.19***	1.16	1.13	1.11	1.19	1.10	1.09	1.19	1.16	1.18	1.09	1.08	1.11	1.16	1.19
average	1.20	1.18	1.17	1.15	1.12	1.12	1.10	1.09	1.16	1.14	1.11	1.07	1.04	1.06	1.08	1.07

* The area that radiation dose measurement by TLD was made.

Table II. The optical density of radiographic film at various points on the cone surface starting from the cone end up to the distance of 8 cm from the cone end of the cone diameter 4.5 cm with bevel end.

a) For 6 MeV

Distance from cone end	Collimator angle related to the point on the surface of IORTcone															
	0°	26°	52°	78°	90°	104°	130°	156°	180°	208°	234°	260°	270°	286°	308°	334°
8 cm	1.30	1.32	1.37	**1.39***	**1.43***	1.36	1.33	1.30	1.26	1.24	1.22	1.23	1.28	1.27	1.27	1.29
7 cm	1.27	1.29	1.35	1.36	1.40	1.34	1.31	1.28	1.24	1.22	1.20	1.21	1.27	1.25	1.24	1.27
6 cm	1.25	1.27	1.33	**1.33***	**1.38***	1.31	1.29	1.25	1.21	1.21	1.18	1.20	1.25	1.23	1.22	1.26
5 cm	1.23	1.25	1.30	1.31	1.34	1.28	1.26	1.23	1.20	1.90	1.17	1.18	1.22	1.21	1.21	1.23
4 cm	1.21	1.22	1.28	**1.29***	**1.30***	1.25	1.24	1.21	1.18	1.17	1.15	1.17	1.20	1.19	1.19	1.20
3 cm	1.19	1.20	1.28	1.26	1.28	1.24	1.22	1.19	1.15	1.15	1.13	1.14	1.17	1.16	1.17	1.17
2 cm	1.16	1.19	1.22	**1.29***	**1.26***	1.22	1.20	1.17	1.14	1.14	1.12	1.12	1.15	1.14	1.15	1.16
1 cm	1.14	1.17	1.21	1.25	1.34	1.23	1.18	1.16	1.13	1.12	1.11	1.10	1.13	1.12	1.13	1.14
0 cm	1.16	1.19	1.22	1.23	**1.29***	**1.24***	1.21	1.16	1.14	1.12	1.10	1.10	1.10	1.10	1.12	1.13
average	1.21	1.23	1.28	1.30	1.34	1.27	1.25	1.22	1.18	1.25	1.15	1.16	1.20	1.19	1.19	1.21

* The area that radiation dose measurement by TLD was made.

b) For 12 MeV.

Distance from cone end	Collimator angle related to the point on the surface of IORTcone															
	0°	26°	52°	78°	90°	104°	130°	156°	180°	208°	234°	260°	270°	286°	308°	334°
8 cm	1.36	1.40	1.40	**1.40***	**1.47***	1.39	1.30	1.27	1.22	1.21	1.20	1.22	1.26	1.27	1.28	1.34
7 cm	1.33	1.38	1.37	1.37	1.43	1.36	1.27	1.23	1.20	1.20	1.19	1.21	1.23	1.24	1.26	1.31
6 cm	1.31	1.34	1.34	**1.34***	**1.39***	1.33	1.25	1.21	1.19	1.18	1.17	1.19	1.21	1.23	1.24	1.28
5 cm	1.28	1.32	1.32	1.31	1.36	1.30	1.24	1.20	1.16	1.16	1.15	1.17	1.19	1.20	1.22	1.26
4 cm	1.25	1.29	**1.29***	1.27	**1.33***	1.28	1.21	1.18	1.15	1.14	1.14	1.15	1.17	1.18	1.19	1.24
3 cm	1.23	1.26	1.27	1.25	1.30	1.25	1.19	1.16	1.13	1.12	1.12	1.13	1.15	1.17	1.18	1.21
2 cm	1.21	1.23	1.24	**1.25***	**1.27***	1.23	1.17	1.15	1.11	1.11	1.09	1.13	1.13	1.13	1.15	1.19
1 cm	1.20	1.24	1.30	1.29	1.25	1.22	1.15	1.13	1.09	1.09	1.09	1.13	1.11	1.13	1.13	1.17
0 cm	1.20	1.22	**1.28***	1.26	**1.28***	1.26	1.15	1.11	1.11	1.08	1.08	1.07	1.10	1.11	1.14	1.16
average	1.26	1.29	1.32	1.31	1.34	1.29	1.21	1.18	1.15	1.14	1.14	1.16	1.17	1.18	1.20	1.24

* The area that radiation dose measurement by TLD was made.

c) For 20 MeV.

Distance from cone end	Collimator angle related to the point on the surface of IORTcone															
	0°	26°	52°	78°	90°	104°	130°	156°	180°	208°	234°	260°	270°	286°	308°	334°
8 cm	1.32	1.38	1.41	**1.43***	**1.49***	1.41	1.36	1.33	1.25	1.23	1.20	1.21	1.22	1.23	1.24	1.30
7 cm	1.28	1.34	1.35	1.38	1.45	1.36	1.33	1.30	1.22	1.20	1.17	1.18	1.20	1.20	1.21	1.26
6 cm	1.24	1.30	1.32	**1.34***	**1.40***	1.33	1.30	1.26	1.19	1.16	1.15	1.16	1.17	1.17	1.19	1.23
5 cm	1.21	1.26	1.28	1.30	1.37	1.30	1.27	1.23	1.17	1.14	1.12	1.13	1.14	1.15	1.15	1.19
4 cm	1.19	1.23	1.25	1.26	**1.33***	**1.27***	1.24	1.19	1.15	1.12	1.09	1.11	1.13	1.12	1.13	1.16
3 cm	1.16	1.21	1.22	1.24	1.29	1.24	1.21	1.17	1.12	1.10	1.07	1.08	1.09	1.09	1.10	1.14
2 cm	1.14	1.18	1.20	**1.21***	**1.26***	1.21	1.18	1.14	1.10	1.07	1.05	1.05	1.07	1.07	1.08	1.11
1 cm	1.12	1.15	1.17	1.20	1.24	1.19	1.16	1.12	1.08	1.06	1.04	1.04	1.05	1.05	1.06	1.09
0 cm	1.12	1.15	1.18	**1.21***	**1.25***	1.19	1.15	1.11	1.09	1.05	1.04	1.03	1.04	1.05	1.07	1.08
average	1.20	1.24	1.26	1.29	1.34	1.28	1.24	1.21	1.15	1.13	1.10	1.11	1.12	1.13	1.14	1.17

* The area that radiation dose measurement by TLD was made.

Table III. The optical density of radiographic film at various points on the cone surface starting from the cone end up to the distance of 8 cm from the cone end of the cone diameter 6.4 cm with flat end.

a) For 6 MeV.

Distance from cone end	Collimator angle related to the point on the surface of IORT cone																			
	0°	18°	36°	54°	72°	90°	108°	126°	144°	162°	180°	198°	216°	234°	252°	270°	288°	306°	324°	342°
8 cm	1.32	1.34	1.37	1.39	1.41	**1.28***	**1.42***	1.41	1.39	1.38	1.35	1.35	1.34	1.33	1.35	1.33	1.29	1.29	1.30	1.31
7 cm	1.30	1.32	1.34	1.36	1.39	1.39	1.39	1.39	1.38	1.36	1.32	1.31	1.32	1.30	1.33	1.30	1.27	1.27	1.28	1.29
6 cm	1.29	1.30	1.32	1.34	**1.37***	**1.36***	1.36	1.36	1.36	1.33	1.31	1.29	1.31	1.28	1.30	1.28	1.26	1.26	1.27	1.28
5 cm	1.27	1.28	1.30	1.32	1.35	1.33	1.35	1.34	1.33	1.30	1.28	1.27	1.26	1.26	1.28	1.26	1.24	1.24	1.24	1.26
4 cm	1.25	1.26	1.29	1.31	1.32	**1.32***	**1.33***	1.29	1.29	1.27	1.26	1.25	1.24	1.23	1.23	1.24	1.19	1.22	1.23	1.24
3 cm	1.23	1.25	1.27	1.28	1.30	1.29	1.29	1.28	1.27	1.25	1.23	1.21	1.22	1.21	1.24	1.23	1.22	1.19	1.23	1.24
2 cm	1.20	1.22	1.24	1.27	1.26	**1.28***	**1.27***	1.25	1.25	1.23	1.22	1.18	1.21	1.19	1.22	1.20	1.21	1.18	1.20	1.20
1 cm	1.24	1.24	1.25	1.25	1.27	1.27	1.28	1.26	1.25	1.23	1.20	1.21	1.20	1.21	1.20	1.18	1.18	1.20	1.20	1.22
0 cm	1.23	1.20	1.23	1.28	1.28	**1.29***	**1.29***	1.29	1.23	1.24	1.20	1.21	1.21	1.22	1.22	1.20	1.21	1.20	1.19	1.23
average	1.26	1.27	1.29	1.31	1.33	1.33	1.33	1.32	1.31	1.29	1.26	1.25	1.25	1.25	1.26	1.25	1.23	1.23	1.24	1.27

* The area that radiation dose measurement by TLD was made.

b) For 12 MeV.

Distance from cone end	Collimator angle related to the point on the surface of IORT cone																			
	0°	18°	36°	54°	72°	90°	108°	126°	144°	162°	180°	198°	216°	234°	252°	270°	288°	306°	324°	342°
8 cm	1.52	1.55	1.56	1.54	1.57	1.53	**1.60***	**1.59***	1.58	1.56	1.53	1.46	1.44	1.45	1.45	1.45	1.45	1.45	1.49	1.50
7 cm	1.48	1.53	1.52	1.49	1.52	1.53	1.56	1.56	1.55	1.53	1.51	1.44	1.43	1.42	1.42	1.43	1.42	1.43	1.46	1.49
6 cm	1.47	1.51	1.49	1.48	1.50	1.51	1.51	**1.53***	**1.53***	1.51	1.48	1.40	1.41	1.39	1.40	1.41	1.40	1.41	1.42	1.47
5 cm	1.45	1.47	1.43	1.47	1.47	1.49	1.49	1.50	1.50	1.48	1.46	1.39	1.38	1.37	1.39	1.39	1.37	1.38	1.39	1.40
4 cm	1.42	1.44	1.44	1.46	1.45	1.46	**1.48***	1.47	**1.48***	1.46	1.44	1.37	1.36	1.35	1.36	1.37	1.34	1.36	1.38	1.39
3 cm	1.37	1.41	1.41	1.42	1.40	1.44	1.45	1.45	1.45	1.44	1.41	1.34	1.34	1.33	1.34	1.35	1.33	1.33	1.37	1.38
2 cm	1.37	1.41	1.38	1.37	1.38	1.42	1.42	**1.44***	**1.43***	1.41	1.40	1.33	1.33	1.31	1.32	1.32	1.31	1.32	1.34	1.37
1 cm	1.37	1.40	1.38	1.36	1.40	1.38	1.40	1.42	1.43	1.42	1.40	1.32	1.32	1.32	1.33	1.30	1.31	1.31	1.33	1.35
0 cm	1.38	1.40	1.40	1.37	1.42	1.35	1.40	**1.45***	**1.45***	1.41	1.40	1.33	1.33	1.33	1.34	1.32	1.33	1.31	1.34	1.34
average	1.43	1.46	1.45	1.44	1.46	1.46	1.48	1.49	1.49	1.47	1.45	1.38	1.37	1.37	1.36	1.37	1.36	1.37	1.39	1.41

* The area that radiation dose measurement by TLD was made.

c) For 20 MeV.

Distance from cone end	Collimator angle related to the point on the surface of IORT cone																			
	0°	18°	36°	54°	72°	90°	108°	126°	144°	162°	180°	198°	216°	234°	252°	270°	288°	306°	324°	342°
8 cm	1.50	1.50	1.55	1.53	**1.56***	**1.56***	1.54	1.51	1.50	1.48	1.45	1.41	1.36	1.36	1.35	1.36	1.37	1.41	1.45	1.46
7 cm	1.47	1.47	1.52	1.49	1.52	1.53	1.51	1.48	1.47	1.45	1.43	1.38	1.34	1.33	1.32	1.33	1.34	1.37	1.41	1.43
6 cm	1.43	1.46	1.48	1.46	**1.50***	**1.49***	1.48	1.46	1.44	1.42	1.40	1.34	1.32	1.30	1.30	1.30	1.32	1.35	1.38	1.40
5 cm	1.39	1.44	1.43	1.44	1.47	1.47	1.45	1.43	1.41	1.39	1.37	1.32	1.30	1.29	1.28	1.29	1.30	1.33	1.35	1.37
4 cm	1.36	1.41	1.41	1.41	**1.43***	**1.44***	1.42	1.41	1.38	1.35	1.34	1.31	1.26	1.26	1.25	1.26	1.27	1.30	1.32	1.35
3 cm	1.31	1.36	1.40	1.39	1.41	1.43	1.40	1.38	1.38	1.35	1.30	1.31	1.25	1.23	1.23	1.23	1.25	1.28	1.31	1.31
2 cm	1.30	1.33	1.37	1.37	**1.38***	**1.40***	1.38	1.38	1.36	1.32	1.29	1.27	1.24	1.22	1.21	1.22	1.23	1.26	1.28	1.29
1 cm	1.32	1.31	1.34	1.36	1.38	1.40	1.38	1.34	1.35	1.31	1.27	1.22	1.22	1.21	1.21	1.22	1.25	1.24	1.26	1.28
0 cm	1.34	1.33	1.37	1.36	**1.39***	**1.40***	1.39	1.35	1.37	1.30	1.27	1.20	1.24	1.23	1.20	1.24	1.23	1.28	1.30	1.30
average	1.38	1.40	1.43	1.42	1.45	1.46	1.44	1.42	1.41	1.37	1.35	1.31	1.28	1.27	1.26	1.27	1.27	1.31	1.34	1.35

* The area that radiation dose measurement by TLD was made.

Table IV. The optical density of radiographic film at various points on the cone surface starting from the cone end up to the distance of 8 cm from the cone end of the cone diameter 6.4 cm with bevel end.

a) For 6 MeV.

Distance from cone end	Collimator angle related to the point on the surface of IORT cone																			
	0°	18°	36°	54°	72°	90°	108°	126°	144°	162°	180°	198°	216°	234°	252°	270°	288°	306°	324°	342°
8 cm	1.40	**1.41***	**1.41***	1.40	1.39	1.41	1.34	1.34	1.36	1.38	1.36	1.34	1.32	1.37	1.38	1.36	1.36	1.31	1.40	1.40
7 cm	1.37	1.39	1.38	1.39	1.38	1.37	1.32	1.32	1.34	1.35	1.34	1.33	1.30	1.35	1.35	1.34	1.34	1.29	1.37	1.38
6 cm	1.34	1.36	**1.37***	**1.37***	1.35	1.36	1.30	1.30	1.31	1.33	1.32	1.30	1.26	1.34	1.33	1.32	1.32	1.25	1.33	1.36
5 cm	1.32	1.33	1.32	1.34	1.33	1.34	1.29	1.29	1.27	1.31	1.28	1.27	1.27	1.31	1.31	1.28	1.30	1.22	1.31	1.32
4 cm	1.30	1.31	**1.31***	**1.32***	1.30	1.32	1.27	1.26	1.25	1.29	1.26	1.23	1.25	1.29	1.28	1.26	1.26	1.20	1.28	1.31
3 cm	1.27	1.29	1.29	1.30	1.29	1.29	1.25	1.24	1.24	1.27	1.23	1.22	1.24	1.27	1.26	1.24	1.24	1.18	1.24	1.28
2 cm	1.25	1.26	**1.27***	**1.27***	1.27	1.27	1.23	1.23	1.22	1.24	1.20	1.21	1.21	1.24	1.23	1.21	1.22	1.16	1.22	1.25
1 cm	1.23	1.24	1.24	1.25	1.24	1.23	1.20	1.21	1.20	1.21	1.17	1.19	1.20	1.21	1.21	1.19	1.19	1.14	1.20	1.23
0 cm	1.20	**1.22***	1.21	**1.23***	1.21	1.22	1.18	1.19	1.16	1.17	1.14	1.12	1.19	1.20	1.19	1.18	1.17	1.13	1.18	1.20
average	1.30	1.31	1.31	1.32	1.31	1.31	1.26	1.26	1.26	1.28	1.28	1.25	1.25	1.29	1.29	1.28	1.27	1.21	1.28	1.30

* The area that radiation dose measurement by TLD was made.

b) For 12 MeV.

Distance from cone end	Collimator angle related to the point on the surface of IORT cone																			
	0°	18°	36°	54°	72°	90°	108°	126°	144°	162°	180°	198°	216°	234°	252°	270°	288°	306°	324°	342°
8 cm	1.63	1.67	1.65	1.69	1.69	1.71	1.70	1.73	1.72	**1.74***	1.72	**1.73***	1.72	1.72	1.68	1.58	1.61	1.61	1.61	1.63
7 cm	1.61	1.63	1.62	1.65	1.66	1.69	1.68	1.70	1.68	1.71	1.70	1.71	1.69	1.70	1.64	1.55	1.59	1.58	1.59	1.61
6 cm	1.58	1.60	1.59	1.62	1.63	1.65	1.64	1.67	1.65	**1.69***	**1.67***	1.67	1.67	167	1.61	1.52	1.55	1.54	1.54	1.57
5 cm	1.54	1.57	1.57	1.59	1.59	1.61	1.61	1.65	1.63	1.65	1.64	1.65	1.63	1.64	1.59	1.50	1.53	1.52	1.52	1.53
4 cm	1.52	1.54	1.53	1.55	1.56	1.60	1.57	1.62	1.60	**1.62***	**1.62***	1.62	1.61	1.61	1.57	1.48	1.50	1.51	1.49	1.51
3 cm	1.49	1.52	1.50	1.52	1.53	1.55	1.55	1.58	1.57	1.58	1.59	1.60	1.58	1.59	1.55	1.44	1.47	1.48	1.47	1.48
2 cm	1.47	1.49	1.47	1.49	1.50	1.52	1.52	1.54	1.55	1.56	**1.57***	**1.58***	1.56	1.56	1.52	1.43	1.45	1.45	1.44	1.46
1 cm	1.42	1.47	1.45	1.46	1.48	1.50	1.50	1.52	1.52	1.56	1.54	1.55	1.54	1.53	1.50	1.42	1.42	1.43	1.42	1.42
0 cm	1.41	1.42	1.42	1.44	1.45	1.47	1.47	1.48	1.51	1.52	**1.53***	**1.53***	1.53	1.52	1.47	1.41	1.41	1.41	1.39	1.40
average	1.52	1.55	1.53	1.56	1.57	1.59	1.58	1.61	1.60	1.63	1.62	1.63	1.61	1.62	1.57	1.48	1.50	1.50	1.50	1.51

* The area that radiation dose measurement by TLD was made.

c) For 20 MeV.

Distance from cone end	Collimator angle related to the point on the surface of IORT cone																			
	0°	18°	36°	54°	72°	90°	108°	126°	144°	162°	180°	198°	216°	234°	252°	270°	288°	306°	324°	342°
8 cm	1.29	1.37	1.42	1.53	1.62	**1.72***	**1.65***	1.65	1.62	1.56	1.54	1.54	1.53	1.53	1.53	1.56	1.39	1.34	1.30	1.30
7 cm	1.27	1.34	1.38	1.49	1.59	1.66	1.61	1.62	1.58	1.53	1.52	1.51	1.49	1.51	1.50	1.53	1.36	1.31	1.28	1.28
6 cm	1.24	1.32	1.35	1.46	1.54	**1.62***	**1.58***	1.58	1.56	1.51	1.47	1.48	1.46	1.47	1.47	1.48	1.34	1.27	1.26	1.25
5 cm	1.22	1.38	1.34	1.43	1.51	1.59	1.55	1.55	1.52	1.47	1.45	1.46	1.44	1.45	1.45	1.45	1.31	1.26	1.23	1.24
4 cm	1.19	1.25	1.31	1.41	1.48	**1.56***	1.51	**1.53***	1.49	1.45	1.43	1.44	1.41	1.42	1.42	1.42	1.29	1.23	1.21	1.21
3 cm	1.18	1.22	1.29	1.36	1.45	1.52	1.47	1.49	1.45	1.42	1.40	1.41	1.38	1.39	1.40	1.41	1.27	1.21	1.19	1.19
2 cm	1.15	1.21	1.27	1.34	1.42	**1.49***	**1.45***	1.44	1.40	1.39	1.37	1.38	1.35	1.36	1.37	1.37	1.25	1.19	1.17	1.17
1 cm	1.14	1.19	1.25	1.32	1.39	1.47	1.41	1.40	1.38	1.37	1.37	1.37	1.34	1.35	1.39	1.35	1.23	1.18	1.15	1.14
0 cm	1.13	1.19	1.24	1.30	1.37	**1.42***	**1.38***	1.38	1.38	1.36	1.36	1.34	1.34	1.36	1.36	1.41	1.21	1.17	1.15	1.14
average	1.20	1.26	1.32	1.40	1.49	1.56	1.51	1.52	1.49	1.45	1.43	1.44	1.42	1.32	1.43	1.44	1.29	1.24	1.22	1.21

* The area that radiation dose measurement by TLD was made.

Table V. The optical density of radiographic film at various points on the cone surface starting from the cone end up to the distance of 8 cm from the cone end of the cone diameter 8.3 cm with flat end.

a) For 6 MeV.

Distance from cone end	**Collimator angle related to the point on the surface of IORT cone**																
	0°	14°	24°	42°	56°	70°	84°	90°	98°	112°	126°	140°	154°	168°	180°	192°	206°
8 cm	1.53	1.57	1.60	**1.61***	**1.62***	1.61	1.61	1.60	1.59	1.58	1.56	1.54	1.50	1.46	1.40	1.38	1.36
7 cm	1.51	1.54	1.57	1.58	1.59	1.58	1.58	1.56	1.56	1.55	1.53	1.50	1.46	1.43	1.38	1.35	1.33
6 cm	1.49	1.52	1.55	**1.56***	**1.56***	1.55	1.55	1.53	1.53	1.51	1.50	1.47	1.43	1.41	1.35	1.32	1.30
5 cm	1.47	1.51	1.54	1.55	1.54	1.53	1.53	1.52	1.49	1.50	1.47	1.45	1.41	1.37	1.32	1.30	1.27
4 cm	1.45	1.49	1.51	**1.52***	**1.52***	1.51	1.51	1.50	1.48	1.46	1.44	1.42	1.39	1.35	1.31	1.28	1.26
3 cm	1.43	1.47	1.49	1.51	1.50	1.48	1.48	1.48	1.46	1.44	1.43	1.39	1.35	1.34	1.28	1.25	1.23
2 cm	1.40	1.44	1.46	**1.47***	**1.47***	1.44	1.45	1.45	1.44	1.42	1.41	1.38	1.34	1.30	1.25	1.23	1.21
1 cm	1.41	1.43	1.47	1.47	1.46	1.47	1.48	1.45	1.44	1.42	1.38	1.35	1.31	1.29	1.26	1.23	1.22
0 cm	1.44	1.46	1.49	**1.51***	**1.51***	1.46	1.50	1.50	1.48	1.46	1.42	1.39	1.35	1.33	1.28	1.25	1.25
average	1.46	1.49	1.52	1.53	1.53	1.51	1.52	1.51	1.50	1.48	1.46	1.43	1.39	1.36	1.31	1.29	1.27

* The area that radiation dose measurement by TLD was made.

a) For 6 MeV (Continued).

Distance from cone end	Collimator angle related to the point on the surface of IORT cone										
	220°	234°	248°	262°	270°	276°	290°	304°	318°	332°	346°
8 cm	1.36	1.35	1.35	1.36	1.37	1.38	1.41	1.45	1.48	1.51	1.56
7 cm	1.33	1.33	1.33	1.35	1.35	1.37	1.40	1.41	1.47	1.50	1.53
6 cm	1.30	1.30	1.29	1.31	1.33	1.33	1.37	1.37	1.43	1.47	1.48
5 cm	1.27	1.27	1.26	1.28	1.31	1.31	1.35	1.36	1.39	1.45	1.48
4 cm	1.26	1.26	1.25	1.27	1.28	1.29	1.32	1.34	1.36	1.41	1.46
3 cm	1.23	1.24	1.24	1.24	1.25	1.27	1.29	1.33	1.36	1.39	1.41
2 cm	1.21	1.21	1.21	1.22	1.23	1.24	1.26	1.27	1.33	1.38	1.40
1 cm	1.22	1.23	1.22	1.23	1.24	1.25	1.28	1.29	1.30	1.36	1.40
0 cm	1.25	1.23	1.24	1.24	1.22	1.23	1.28	1.30	1.32	1.36	1.43
average	1.27	1.27	1.27	1.28	1.29	1.30	1.33	1.35	1.38	1.43	1.46

* The area that radiation dose measurement by TLD was made.

b) For 12 MeV.

Distance from cone end	Collimator angle related to the point on the surface of IORT cone																
	0°	14°	24°	42°	56°	70°	84°	90°	98°	112°	126°	140°	154°	168°	180°	192°	206°
8 cm	1.67	1.73	**1.75***	**1.76***	1.75	1.74	1.72	1.68	1.66	1.61	1.56	1.52	1.49	1.42	1.43	1.39	1.38
7 cm	1.64	1.70	1.73	1.74	1.72	1.71	1.68	1.66	1.62	1.59	1.53	1.49	1.47	1.40	1.39	1.38	1.37
6 cm	1.63	1.67	**1.70***	**1.70***	1.69	1.68	1.65	1.62	1.60	1.56	1.50	1.47	1.44	1.39	1.36	1.37	1.34
5 cm	1.60	1.66	1.67	1.67	1.67	1.66	1.64	1.60	1.57	1.54	1.48	1.46	1.40	1.38	1.34	1.33	1.32
4 cm	1.57	1.62	**1.65***	**1.65***	1.64	1.63	1.61	1.58	1.55	1.51	1.45	1.44	1.39	1.35	1.33	1.31	1.30
3 cm	1.54	1.61	1.63	1.62	1.62	1.60	1.58	1.56	1.52	1.49	1.42	1.40	1.36	1.34	1.33	1.30	1.28
2 cm	1.53	1.58	**1.60***	**1.60***	1.59	1.59	1.55	1.52	1.50	1.46	1.42	1.39	1.35	1.30	1.30	1.28	1.26
1 cm	1.54	1.57	1.59	1.60	1.60	1.58	1.57	1.55	1.51	1.45	1.40	1.38	1.33	1.32	1.31	1.29	1.27
0 cm	1.53	1.58	**1.63***	**1.63***	1.62	1.62	1.60	1.57	1.54	1.48	1.47	1.40	1.39	1.33	1.34	1.30	1.29
average	1.58	1.64	1.66	1.66	1.66	1.65	1.62	1.59	1.56	1.52	1.47	1.44	1.40	1.36	1.35	1.33	1.31

* The area that radiation dose measurement by TLD was made.

b) For 12 MeV (Continued).

Distance from cone end	Collimator angle related to the point on the surface of IORT cone										
	220°	234°	248°	262°	270°	276°	290°	304°	318°	332°	346°
8 cm	1.38	1.38	1.38	1.40	1.42	1.45	1.49	1.53	1.56	1.60	1.65
7 cm	1.36	1.36	1.37	1.37	1.40	1.43	1.47	1.50	1.54	1.58	1.62
6 cm	1.34	1.34	1.35	1.35	1.38	1.41	1.43	1.48	1.51	1.55	1.60
5 cm	1.32	1.32	1.33	1.33	1.36	1.39	1.41	1.46	1.49	1.53	1.57
4 cm	1.31	1.30	1.30	1.31	1.34	1.37	1.39	1.44	1.47	1.49	1.54
3 cm	1.27	1.28	1.28	1.29	1.33	1.35	1.38	1.42	1.45	1.48	1.52
2 cm	1.26	1.26	1.28	1.29	1.31	1.33	1.36	1.39	1.43	1.46	1.49
1 cm	1.28	1.27	1.28	1.30	1.31	1.33	1.37	1.40	1.44	1.47	1.50
0 cm	1.29	1.31	1.31	1.33	1.33	1.36	1.38	1.44	1.47	1.49	1.50
average	1.31	1.31	1.32	1.33	1.35	1.38	1.41	1.45	1.48	1.52	1.55

* The area that radiation dose measurement by TLD was made.

c) For 20 MeV.

Distance from cone end	Collimator angle related to the point on the surface of IORT cone																
	0°	14°	24°	42°	56°	70°	84°	90°	98°	112°	126°	140°	154°	168°	180°	192°	206°
8 cm	1.79	1.82	1.83	**1.73***	**1.84***	1.82	1.81	1.81	1.78	1.76	1.77	1.75	1.73	1.69	1.70	1.70	1.69
7 cm	1.75	1.78	1.81	1.81	1.80	1.79	1.77	1.78	1.77	1.75	1.74	1.72	1.69	1.66	1.66	1.66	1.66
6 cm	1.74	1.77	1.79	**1.81***	**1.79***	1.77	1.76	1.77	1.76	1.73	1.72	1.69	1.66	1.63	1.64	1.63	1.62
5 cm	1.70	1.74	1.76	1.77	1.79	1.75	1.73	1.75	1.73	1.71	1.70	1.66	1.63	1.61	1.61	1.60	1.61
4 cm	1.68	1.71	1.69	**1.73***	**1.73***	1.72	1.71	1.72	1.70	1.69	1.66	1.65	1.61	1.57	1.56	1.56	1.57
3 cm	1.63	1.66	1.67	1.68	1.69	1.65	1.66	1.68	1.66	1.65	1.64	1.60	1.57	1.54	1.53	1.53	1.54
2 cm	1.60	1.62	1.64	**1.66***	**1.67***	1.62	1.62	1.65	1.63	1.62	1.61	1.58	1.54	1.52	1.52	1.50	1.53
1 cm	1.60	1.64	1.64	1.64	1.67	1.64	1.62	1.65	1.63	1.61	1.61	1.59	1.55	1.51	1.50	1.50	1.52
0 cm	1.66	1.73	1.74	**1.76***	**1.74***	1.73	1.69	1.74	1.72	1.68	1.65	1.64	1.60	1.60	1.54	1.52	1.55
average	1.68	1.72	1.73	1.74	1.75	1.72	1.71	1.73	1.71	1.69	1.68	1.65	1.62	1.59	1.58	1.58	1.59

* The area that radiation dose measurement by TLD was made.

c) For 20 MeV (Continued).

Distance from cone end	**Collimator angle related to the point on the surface of IORT cone**										
	220°	234°	248°	262°	270°	276°	290°	304°	318°	332°	346°
8 cm	1.65	1.68	1.58	1.62	1.62	1.63	1.65	1.65	1.68	1.72	1.76
7 cm	1.61	1.65	1.56	1.58	1.57	1.58	1.59	1.61	1.64	1.69	1.71
6 cm	1.59	1.62	1.53	1.54	1.54	1.56	1.54	1.60	1.62	1.67	1.70
5 cm	1.57	1.59	1.50	1.51	1.50	1.52	1.53	1.58	1.58	1.62	1.67
4 cm	1.54	1.55	1.47	1.48	1.48	1.49	1.51	1.53	1.54	1.58	1.63
3 cm	1.50	1.53	1.44	1.44	1.46	1.46	1.47	1.46	1.50	1.53	1.58
2 cm	1.49	1.52	1.41	1.42	1.44	1.44	1.45	1.45	1.49	1.49	1.54
1 cm	1.45	1.50	1.43	1.42	1.41	1.43	1.44	1.44	1.44	1.50	1.55
0 cm	1.47	1.52	1.48	1.50	1.46	1.48	1.50	1.52	1.52	1.59	1.62
average	1.54	1.57	1.49	1.50	1.50	1.51	1.52	1.54	1.56	1.60	1.64

* The area that radiation dose measurement by TLD was made.

Table VI. The optical density of radiographic film at various points on the cone surface starting from the cone end up to the distance of 8 cm from the cone end of the cone diameter 8.3 cm with bevel end.

a) For 6 MeV.

Distance from cone end	**Collimator angle related to the point on the surface of IORT cone**																
	0°	14°	24°	42°	56°	70°	84°	90°	98°	112°	126°	140°	154°	168°	180°	192°	206°
8 cm	1.31	1.32	1.34	1.35	1.38	1.40	1.44	**1.46***	**1.45***	1.44	1.41	1.40	1.38	1.34	1.30	1.29	1.26
7 cm	1.29	1.30	1.32	1.35	1.36	1.38	1.42	1.45	1.43	1.42	1.39	1.38	1.36	1.32	1.28	1.26	1.25
6 cm	1.27	1.29	1.30	1.33	1.35	1.37	1.40	**1.43***	**1.41***	1.40	1.37	1.36	1.34	1.30	1.27	1.25	1.23
5 cm	1.27	1.27	1.29	1.31	1.33	1.35	1.39	1.42	1.40	1.39	1.36	1.34	1.33	1.29	1.25	1.24	1.21
4 cm	1.25	1.26	1.28	1.30	1.32	1.34	1.37	**1.39***	**1.37***	1.37	1.35	1.33	1.32	1.27	1.23	1.23	1.20
3 cm	1.24	1.26	1.27	1.29	1.30	1.32	1.35	1.37	1.36	1.36	1.34	1.32	1.30	1.26	1.21	1.21	1.19
2 cm	1.22	1.25	1.25	1.28	1.28	1.30	1.34	**1.36***	**1.35***	1.35	1.32	1.30	1.29	1.24	1.21	1.19	1.19
1 cm	1.21	1.24	1.24	1.27	1.28	1.30	1.32	1.34	1.34	1.33	1.31	1.29	1.26	1.22	1.20	1.16	1.19
0 cm	1.21	1.23	1.23	1.26	1.26	1.32	1.32	1.33	**1.35***	**1.34***	1.33	1.31	1.24	1.19	1.21	1.15	1.20
average	1.25	1.27	1.28	1.30	1.32	1.34	1.37	1.39	1.38	1.38	1.35	1.34	1.31	1.27	1.24	1.22	1.21

* The area that radiation dose measurement by TLD was made.

a) For 6 MeV (Continued).

Distance from cone end	**Collimator angle related to the point on the surface of IORT cone**										
	220°	234°	248°	262°	270°	276°	290°	304°	318°	332°	346°
8 cm	1.26	1.26	1.27	1.28	1.27	1.31	1.29	1.27	1.28	1.28	1.30
7 cm	1.26	1.25	1.26	1.27	1.27	1.30	1.28	1.26	1.28	1.28	1.28
6 cm	1.25	1.24	1.24	1.25	1.25	1.28	1.26	1.25	1.25	1.26	1.27
5 cm	1.23	1.22	1.23	1.23	1.23	1.27	1.25	1.24	1.25	1.25	1.26
4 cm	1.20	1.20	1.21	1.22	1.21	1.25	1.24	1.23	1.23	1.24	1.25
3 cm	1.19	1.19	1.20	1.21	1.20	1.24	1.22	1.21	1.23	1.22	1.23
2 cm	1.18	1.18	1.19	1.20	1.19	1.22	1.21	1.20	1.21	1.21	1.22
1 cm	1.18	1.18	1.18	1.18	1.18	1.22	1.20	1.19	1.20	1.20	1.21
0 cm	1.19	1.19	1.17	1.18	1.19	1.21	1.20	1.20	1.18	1.19	1.20
average	1.22	1.21	1.22	1.22	1.22	1.26	1.24	1.23	1.23	1.24	1.25

* The area that radiation dose measurement by TLD was made.

b) For 12 MeV.

Distance from cone end	Collimator angle related to the point on the surface of IORT cone																
	0°	14°	24°	42°	56°	70°	84°	90°	98°	112°	126°	140°	154°	168°	180°	192°	206°
8 cm	1.43	1.45	1.46	1.49	1.50	1.51	1.54	1.54	**1.61***	**1.59***	1.57	1.56	1.55	1.53	1.50	1.50	1.47
7 cm	1.41	1.43	1.44	1.47	1.49	1.49	1.52	1.54	1.60	1.58	1.56	1.55	1.53	1.51	1.49	1.48	1.45
6 cm	1.39	1.42	1.43	1.46	1.47	1.48	1.51	1.52	**1.58***	**1.57***	1.54	1.53	1.52	1.49	1.48	1.46	1.43
5 cm	1.38	1.40	1.41	1.44	1.45	1.46	1.48	1.50	1.59	1.55	1.52	1.51	1.51	1.47	1.45	1.44	1.42
4 cm	1.36	1.39	1.40	1.42	1.44	1.45	1.46	1.49	**1.58***	**1.53***	1.50	1.48	1.48	1.45	1.43	1.43	1.39
3 cm	1.35	1.37	1.38	1.41	1.42	1.44	1.45	1.47	1.52	1.51	1.48	1.47	1.46	1.43	1.42	1.40	1.36
2 cm	1.33	1.36	1.37	1.40	1.41	1.42	1.43	1.46	**1.50***	**1.48***	1.47	1.46	1.44	1.41	1.41	1.39	1.36
1 cm	1.33	1.35	1.37	1.38	1.40	1.41	1.42	1.44	1.48	1.48	1.46	1.43	1.43	1.40	1.40	1.39	1.35
0 cm	1.32	1.35	1.36	1.37	1.40	1.41	1.40	1.43	**1.46***	**1.46***	1.44	1.41	1.39	1.38	1.40	1.38	1.36
average	1.37	1.39	1.41	1.43	1.44	1.45	1.47	1.49	1.55	1.53	1.50	1.50	1.48	1.45	1.44	1.43	1.40

* The area that radiation dose measurement by TLD was made.

b) For 12 MeV (Continued).

Distance from cone end	**Collimator angle related to the point on the surface of IORT cone**										
	220°	234°	248°	262°	270°	276°	290°	304°	318°	332°	346°
8 cm	1.44	1.41	1.40	1.38	1.37	1.38	1.38	1.37	1.39	1.40	1.42
7 cm	1.43	1.40	1.38	1.37	1.35	1.37	1.36	1.36	1.38	1.38	1.41
6 cm	1.41	1.38	1.37	1.35	1.33	1.36	1.35	1.35	1.36	1.36	1.39
5 cm	1.40	1.36	1.35	1.33	1.31	1.34	1.34	1.34	1.35	1.35	1.37
4 cm	1.37	1.34	1.34	1.32	1.29	1.33	1.32	1.32	1.33	1.34	1.36
3 cm	1.36	1.33	1.32	1.31	1.28	1.32	1.31	1.31	1.32	1.33	1.35
2 cm	1.34	1.32	1.30	1.29	1.27	1.31	1.30	1.29	1.31	1.32	1.33
1 cm	1.34	1.31	1.29	1.28	1.27	1.28	1.29	1.29	1.29	1.31	1.32
0 cm	1.34	1.32	1.30	1.26	1.26	1.29	1.29	1.28	1.29	1.29	1.31
average	1.38	1.35	1.34	1.32	1.30	1.33	1.33	1.32	1.34	1.34	1.36

* The area that radiation dose measurement by TLD was made.

c) For 20 MeV.

Distance from cone end	Collimator angle related to the point on the surface of IORT cone																
	0°	14°	24°	42°	56°	70°	84°	90°	98°	112°	126°	140°	154°	168°	180°	192°	206°
8 cm	1.47	1.49	1.50	1.51	1.53	1.54	1.63	1.65	**1.67***	**1.68***	1.66	1.66	1.65	1.61	1.56	1.54	1.50
7 cm	1.45	1.46	1.48	1.48	1.52	1.51	1.60	1.61	1.64	1.65	1.62	1.63	1.62	1.59	1.54	1.53	1.48
6 cm	1.43	1.45	1.46	1.47	1.49	1.50	1.58	1.58	**1.61***	**1.62***	1.60	1.60	1.61	1.56	1.52	1.50	1.46
5 cm	1.41	1.43	1.44	1.44	1.47	1.48	1.57	1.57	1.59	1.59	1.58	1.57	1.58	1.54	1.50	1.48	1.44
4 cm	1.38	1.42	1.42	1.43	1.45	1.46	1.56	1.55	**1.56***	**1.57***	1.55	1.55	1.55	1.52	1.47	1.46	1.42
3 cm	1.36	1.39	1.40	1.39	1.44	1.44	1.51	1.52	1.54	1.55	1.53	1.52	1.53	1.50	1.45	1.44	1.40
2 cm	1.35	1.37	1.39	1.40	1.42	1.42	1.49	1.50	1.50	**1.53***	**1.51***	1.51	1.51	1.46	1.43	1.40	1.38
1 cm	1.34	1.37	1.38	1.40	1.43	1.42	1.48	1.48	1.49	1.50	1.48	1.48	1.47	1.46	1.42	1.40	1.39
0 cm	1.35	1.37	1.39	1.42	1.44	1.43	1.47	1.47	**1.47***	**1.48***	1.47	1.47	1.46	1.46	1.42	1.40	1.38
average	1.39	1.42	1.43	1.44	1.47	1.47	1.54	1.55	1.56	1.57	1.55	1.55	1.55	1.52	1.48	1.46	1.43

* The area that radiation dose measurement by TLD was made.

c) For 20 MeV (Continued).

Distance from cone end	**Collimator angle related to the point on the surface of IORT cone**										
	220°	234°	248°	262°	270°	276°	290°	304°	318°	332°	346°
8 cm	1.49	1.45	1.42	1.35	1.36	1.38	1.39	1.41	1.45	1.48	1.50
7 cm	1.47	1.42	1.40	1.33	1.34	1.36	1.38	1.39	1.42	1.46	1.48
6 cm	1.44	1.40	1.38	1.30	1.32	1.34	1.35	1.37	1.40	1.44	1.46
5 cm	1.42	1.38	1.36	1.28	1.31	1.32	1.33	1.35	1.38	1.42	1.44
4 cm	1.41	1.36	1.34	1.28	1.28	1.30	1.32	1.33	1.36	1.41	1.43
3 cm	1.39	1.35	1.33	1.27	1.27	1.29	1.31	1.32	1.34	1.40	1.41
2 cm	1.36	1.34	1.31	1.26	1.25	1.29	1.30	1.31	1.34	1.37	1.41
1 cm	1.36	1.33	1.30	1.24	1.23	1.28	1.30	1.32	1.34	1.35	1.38
0 cm	1.35	1.30	1.29	1.22	1.23	1.29	1.32	1.32	1.33	1.34	1.36
average	1.41	1.37	1.35	1.28	1.29	1.32	1.33	1.35	1.37	1.41	1.43

* The area that radiation dose measurement by TLD was made.

Table VII. The optical density of radiographic film at various points on the cone surface starting from the cone end up to the distance of 8 cm from the cone end of the cone diameter 9.5 cm with flat end.

a) For 6 MeV.

Distance from cone end	Collimator angle related to the point on the surface of IORT cone															
	0°	12°	24°	36°	48°	60°	72°	84°	90°	96°	108°	120°	132°	144°	156°	168°
8 cm	1.81	1.82	1.86	1.89	1.89	1.90	1.93	1.92	1.94	1.95	1.97	1.97	**1.96***	**1.97***	1.95	1.93
7 cm	1.79	1.79	1.83	1.86	1.86	1.87	1.89	1.90	1.91	1.91	1.93	1.94	1.94	1.94	1.92	1.91
6 cm	1.77	1.78	1.82	1.82	1.82	1.85	1.86	1.86	1.88	1.89	1.91	1.91	**1.92***	**1.91***	1.90	1.86
5 cm	1.75	1.74	1.79	1.80	1.80	1.81	1.82	1.82	1.85	1.85	1.87	1.88	1.87	1.87	1.88	1.85
4 cm	1.72	1.73	1.75	1.77	1.77	1.77	1.80	1.80	1.82	1.82	1.84	1.83	**1.84***	**1.84***	1.84	1.82
3 cm	1.70	1.69	1.73	1.76	1.76	1.75	1.78	1.78	1.78	1.80	1.81	1.82	1.81	1.80	1.81	1.79
2 cm	1.67	1.69	1.73	1.75	1.75	1.75	1.74	1.74	1.77	1.78	1.79	1.80	**1.80***	**1.81***	1.78	1.76
1 cm	1.64	1.67	1.73	1.75	1.75	1.76	1.76	1.76	1.78	1.77	1.79	1.80	1.81	1.82	1.81	1.78
0 cm	1.66	1.70	1.71	1.76	1.76	1.76	1.75	1.75	1.78	1.81	1.80	**1.84***	**1.82***	1.78	1.81	1.79
average	1.72	1.73	1.77	1.80	1.80	1.80	1.81	1.81	1.83	1.84	1.86	1.87	1.83	1.86	1.86	1.83

* The area that radiation dose measurement by TLD was made.

a) For 6 MeV (Continued).

Distance from cone end	Collimator angle related to the point on the surface of IORT cone															
	180°	192°	204°	216°	228°	240°	252°	264°	270°	276°	288°	300°	312°	324°	336°	348°
8 cm	1.90	1.86	1.82	1.78	1.73	1.68	1.66	1.62	1.61	1.62	1.62	1.64	1.69	1.72	1.76	1.79
7 cm	1.87	1.83	1.78	1.76	1.71	1.68	1.65	1.61	1.61	1.60	1.60	1.62	1.67	1.69	1.73	1.77
6 cm	1.84	1.80	1.77	1.72	1.68	1.67	1.61	1.58	1.58	1.58	1.59	1.61	1.65	1.68	1.71	1.74
5 cm	1.82	1.76	1.75	1.68	1.65	1.63	1.60	1.56	1.57	1.57	1.58	1.59	1.64	1.66	1.69	1.73
4 cm	1.80	1.75	1.72	1.67	1.63	1.61	1.61	1.53	1.54	1.55	1.57	1.58	1.61	1.64	1.67	1.71
3 cm	1.76	1.73	1.69	1.66	1.57	1.57	1.55	1.51	1.53	1.53	1.53	1.56	1.59	1.63	1.65	1.68
2 cm	1.75	1.68	1.66	1.63	1.59	1.56	1.55	1.51	1.50	1.51	1.54	1.54	1.58	1.59	1.63	1.65
1 cm	1.76	1.74	1.67	1.62	1.60	1.54	1.55	1.50	1.48	1.52	1.54	1.56	1.54	1.59	1.62	1.65
0 cm	1.78	1.72	1.65	1.67	1.61	1.60	1.57	1.53	1.52	1.54	1.56	1.56	1.60	1.63	1.64	1.69
average	1.81	1.76	1.72	1.69	1.64	1.62	1.59	1.55	1.55	1.56	1.57	1.58	1.62	1.65	1.68	1.71

* The area that radiation dose measurement by TLD was made.

b) For 12 MeV.

Distance from cone end	Collimator angle related to the point on the surface of IORT cone															
	0°	12°	24°	36°	48°	60°	72°	84°	90°	96°	108°	120°	132°	144°	156°	168°
8 cm	1.79	1.79	1.82	1.85	1.90	1.95	1.98	2.00	**2.01***	**2.00***	2.00	1.99	2.00	1.97	1.95	1.92
7 cm	1.76	1.78	1.81	1.84	1.89	1.92	1.96	1.98	1.99	1.97	1.98	1.97	1.97	1.95	1.93	1.88
6 cm	1.76	1.77	1.80	1.83	1.87	1.91	1.94	**1.97***	**1.97***	1.95	1.97	1.97	1.94	1.93	1.93	1.88
5 cm	1.75	1.76	1.79	1.81	1.86	1.88	1.92	1.94	1.94	1.93	1.94	1.95	1.91	1.91	1.91	1.86
4 cm	1.73	1.74	1.77	1.79	1.83	1.86	1.88	**1.91***	**1.91***	1.90	1.89	1.92	1.89	1.87	1.87	1.84
3 cm	1.67	1.73	1.75	1.77	1.81	1.82	1.85	1.87	1.87	1.84	1.87	1.86	1.88	1.86	1.83	1.82
2 cm	1.64	1.70	1.73	1.76	1.78	1.81	1.83	**1.85***	1.84	**1.85***	1.84	1.84	1.83	1.81	1.78	1.79
1 cm	1.67	1.70	1.74	1.78	1.80	1.83	1.84	1.85	1.85	1.84	1.84	1.85	1.85	1.84	1.82	1.83
0 cm	1.77	1.79	1.82	1.90	1.88	1.94	1.95	1.94	**1.94***	**1.96***	1.92	1.97	1.93	1.89	1.89	1.89
average	1.73	1.75	1.69	1.74	1.79	1.84	1.87	1.90	1.92	1.91	1.92	1.92	1.88	1.86	1.86	1.84

* The area that radiation dose measurement by TLD was made.

b) For 12 MeV (Continued).

Distance from cone end	Collimator angle related to the point on the surface of IORT cone															
	180°	192°	204°	216°	228°	240°	252°	264°	270°	276°	288°	300°	312°	324°	336°	348°
8 cm	1.90	1.77	1.71	1.64	1.58	1.53	1.49	1.46	1.47	1.51	1.57	1.62	1.61	1.71	1.76	1.84
7 cm	1.87	1.74	1.68	1.61	1.55	1.54	1.46	1.45	1.47	1.50	1.57	1.62	1.65	1.69	1.76	1.83
6 cm	1.85	1.71	1.65	1.58	1.54	1.49	1.45	1.43	1.45	1.49	1.55	1.61	1.64	1.70	1.74	1.82
5 cm	1.83	1.68	1.63	1.57	1.52	1.47	1.44	1.42	1.45	1.48	1.54	1.59	1.63	1.68	1.74	1.81
4 cm	1.78	1.66	1.61	1.53	1.49	1.45	1.43	1.40	1.42	1.46	1.52	1.58	1.61	1.66	1.71	1.78
3 cm	1.77	1.64	1.59	1.52	1.48	1.42	1.41	1.40	1.40	1.45	1.50	1.55	1.58	1.64	1.68	1.76
2 cm	1.75	1.63	1.55	1.50	1.46	1.40	1.39	1.38	1.39	1.43	1.47	1.51	1.56	1.61	1.65	1.72
1 cm	1.77	1.66	1.56	1.52	1.45	1.43	1.38	1.39	1.40	1.44	1.49	1.53	1.57	1.61	1.67	1.75
0 cm	1.84	1.80	1.63	1.65	1.54	1.53	1.47	1.50	1.49	1.53	1.60	1.62	1.67	1.72	1.76	1.85
average	1.80	1.71	1.64	1.59	1.54	1.49	1.45	1.43	1.43	1.47	1.53	1.57	1.60	1.65	1.72	1.80

* The area that radiation dose measurement by TLD was made.

c) For 20 MeV.

Distance From cone end	Collimator angle related to the point on the surface of IORT cone															
	0°	12°	24°	36°	48°	60°	72°	84°	90°	96°	108°	120°	132°	144°	156°	168°
8 cm	1.73	1.77	1.80	1.82	1.79	1.83	1.88	1.95	2.02	2.04	**2.06***	2.04	**2.05***	2.03	2.03	2.04
7 cm	1.73	1.77	1.79	1.81	1.78	1.82	1.88	1.95	2.00	2.01	2.03	2.04	2.04	1.99	2.00	2.00
6 cm	1.72	1.75	1.79	1.81	1.78	1.82	1.87	1.91	1.97	1.98	2.01	**2.03***	**2.01***	1.96	1.98	1.99
5 cm	1.71	1.74	1.78	1.80	1.78	1.81	1.87	1.90	1.95	1.96	1.98	2.01	1.97	1.95	1.96	1.96
4 cm	1.70	1.73	1.77	1.79	1.78	1.79	1.86	1.86	1.93	1.95	1.95	**1.96***	**1.96***	1.95	1.94	1.93
3 cm	1.70	1.71	1.76	1.76	1.77	1.78	1.85	1.85	1.91	1.93	1.95	1.93	1.96	1.94	1.90	1.89
2 cm	1.68	1.71	1.74	1.75	1.76	1.76	1.84	1.85	1.84	1.90	1.91	**1.93***	**1.93***	1.92	1.86	1.86
1 cm	1.66	1.69	1.72	1.73	1.76	1.73	1.81	1.85	1.84	1.88	1.90	1.91	1.89	1.87	1.86	1.85
0 cm	1.70	1.70	1.76	1.80	1.82	1.75	1.83	1.83	1.87	1.91	**1.92***	1.91	**1.94***	1.90	1.89	1.87
average	1.70	1.73	1.77	1.79	1.78	1.79	1.85	1.88	1.93	1.95	1.97	1.97	1.97	1.95	1.94	1.93

* The area that radiation dose measurement by TLD was made.

c) For 20 MeV (Continued).

Distance from cone end	Collimator angle related to the point on the surface of IORT cone															
	180°	192°	204°	216°	228°	240°	252°	264°	270°	276°	288°	300°	312°	324°	336°	348°
8 cm	2.02	1.99	1.91	1.85	1.77	1.71	1.66	1.64	1.58	1.55	1.54	1.55	1.58	1.60	1.64	1.71
7 cm	1.99	1.98	1.91	1.82	1.76	1.71	1.66	1.63	1.56	1.54	1.54	1.55	1.58	1.60	1.64	1.70
6 cm	1.96	1.97	1.87	1.82	1.73	1.70	1.65	1.61	1.55	1.53	1.53	1.54	1.57	1.60	1.64	1.70
5 cm	1.94	1.93	1.84	1.78	1.70	1.68	1.62	1.59	1.53	1.53	1.52	1.54	1.56	1.59	1.63	1.69
4 cm	1.91	1.91	1.81	1.77	1.69	1.66	1.60	1.58	1.52	1.52	1.52	1.53	1.55	1.59	1.63	1.68
3 cm	1.87	1.88	1.80	1.75	1.69	1.62	1.58	1.56	1.50	1.50	1.50	1.52	1.55	1.58	1.62	1.67
2 cm	1.83	1.83	1.89	1.73	1.66	1.59	1.58	1.54	1.50	1.48	1.48	1.50	1.54	1.58	1.61	1.66
1 cm	1.83	1.80	1.77	1.70	1.62	1.55	1.56	1.53	1.47	1.46	1.47	1.47	1.53	1.57	1.59	1.65
0 cm	1.85	1.84	1.78	1.72	1.66	1.59	1.56	1.51	1.48	1.48	1.48	1.50	1.55	1.59	1.61	1.66
average	1.96	1.90	1.84	1.77	1.70	1.65	1.61	1.58	1.52	1.51	.151	1.52	1.56	1.59	1.62	1.68

* The area that radiation dose measurement by TLD was made.

Table VIII. The optical density of radiographic film at various points on the cone surface starting from the cone end up to the distance of 8 cm from the cone end of the cone diameter 9.5 cm with bevel end.

a) For 6 MeV.

Distance from cone end	**Collimator angle related to the point on the surface of IORT cone**															
	0°	12°	24°	36°	48°	60°	72°	84°	90°	96°	108°	120°	132°	144°	156°	168°
8 cm	1.71	1.76	1.79	1.80	1.81	1.80	1.85	1.85	1.87	1.90	**1.91***	**1.91***	1.88	1.87	1.81	1.78
7 cm	1.68	1.74	1.74	1.78	1.79	1.79	1.82	1.83	1.85	1.88	1.87	1.88	1.85	1.83	1.78	1.76
6 cm	1.65	1.71	1.71	1.76	1.77	1.77	1.80	1.81	1.82	1.86	**1.86***	**1.86***	1.83	1.81	1.75	1.72
5 cm	1.63	1.68	1.69	1.74	1.75	1.74	1.78	1.78	1.79	1.84	1.84	1.83	1.79	1.77	1.72	1.69
4 cm	1.60	1.66	1.67	1.70	1.70	1.72	1.74	1.75	1.76	1.80	**1.80***	**1.80***	1.76	1.74	1.70	1.66
3 cm	1.57	1.62	1.63	1.67	1.67	1.68	1.71	1.72	1.72	1.76	1.76	1.77	1.73	1.71	1.66	1.63
2 cm	1.55	1.59	1.61	1.64	1.65	1.65	1.68	1.69	1.69	**1.73***	**1.74***	1.71	1.70	1.68	1.63	1.60
1 cm	1.54	1.57	1.59	1.62	1.62	1.63	1.65	1.65	1.67	1.71	1.70	1.70	1.70	1.65	1.66	1.59
0 cm	1.51	1.53	1.55	1.56	1.56	1.59	1.62	1.61	1.65	**1.70***	1.65	**1.72***	1.65	1.62	1.57	1.53
average	1.60	1.65	1.66	1.70	1.70	1.71	1.74	1.74	1.76	1.80	1.79	1.80	1.77	1.74	1.70	1.66

* The area that radiation dose measurement by TLD was made.

a) For 6 MeV (Continued).

Distance from cone end	Collimator angle related to the point on the surface of IORT cone															
	180°	192°	204°	216°	228°	240°	252°	264°	270°	276°	288°	300°	312°	324°	336°	348°
8 cm	1.72	1.70	1.65	1.61	1.56	1.55	1.53	1.50	1.48	1.47	1.49	1.51	1.54	1.59	1.62	1.65
7 cm	1.68	1.67	1.61	1.58	1.54	1.53	1.51	1.48	1.46	1.45	1.47	1.50	1.52	1.56	1.60	1.62
6 cm	1.66	1.63	1.59	1.56	1.50	1.51	1.48	1.46	1.45	1.43	1.46	1.48	1.50	1.54	1.59	1.60
5 cm	1.63	1.61	1.55	1.52	1.48	1.49	1.46	1.43	1.43	1.43	1.43	1.45	1.47	1.52	1.58	1.57
4 cm	1.59	1.58	1.53	1.50	1.46	1.44	1.43	1.42	1.42	1.42	1.42	1.43	1.43	1.50	1.55	1.54
3 cm	1.57	1.56	1.51	1.49	1.41	1.42	1.41	1.40	1.39	1.31	1.40	1.40	1.43	1.48	1.53	1.52
2 cm	1.58	1.53	1.48	1.46	1.42	1.40	1.40	1.40	1.38	1.35	1.38	1.39	1.42	1.45	1.50	1.51
1 cm	1.53	1.51	1.45	1.42	1.36	1.39	1.39	1.40	1.38	1.38	1.37	1.37	1.41	1.42	1.49	1.48
0 cm	1.51	1.46	1.43	1.41	1.33	1.38	1.37	1.35	1.36	1.38	1.40	1.36	1.36	1.38	1.48	1.46
average	1.61	1.58	1.53	1.51	1.45	1.46	1.44	1.43	1.42	1.40	1.42	1.43	1.46	1.49	1.55	1.55

* The area that radiation dose measurement by TLD was made.

b) For 12 MeV.

Distance from cone end	Collimator angle related to the point on the surface of IORT cone															
	0°	12°	24°	36°	48°	60°	72°	84°	90°	96°	108°	120°	132°	144°	156°	168°
8 cm	1.84	1.88	1.89	1.91	1.93	1.94	1.94	**1.98***	**1.98***	1.97	1.97	1.97	1.95	1.93	1.87	1.85
7 cm	1.83	1.87	1.90	1.91	1.93	1.94	1.94	1.95	1.97	1.97	1.97	1.96	1.92	1.89	1.84	1.82
6 cm	1.81	1.86	1.88	1.90	1.92	1.93	1.95	1.95	**1.96***	**1.96***	1.95	1.94	1.90	1.87	1.81	1.79
5 cm	1.79	1.84	1.87	1.91	1.91	1.91	1.94	1.95	1.95	1.94	1.93	1.91	1.86	1.83	1.79	1.76
4 cm	1.78	1.82	1.85	1.88	1.89	1.89	1.92	**1.93***	**1.92***	1.91	1.90	1.88	1.83	1.81	1.76	1.74
3 cm	1.75	1.81	1.84	1.87	1.88	1.88	1.89	1.90	1.91	1.88	1.87	1.85	1.81	1.79	1.74	1.71
2 cm	1.74	1.79	1.81	1.86	1.87	1.87	1.88	**1.89***	**1.89***	1.86	1.84	1.84	1.79	1.77	1.72	1.68
1 cm	1.72	1.78	1.79	1.84	1.84	1.78	1.88	1.88	1.90	1.82	1.83	1.81	1.78	1.75	1.72	1.68
0 cm	1.66	1.71	1.70	1.78	1.77	1.74	1.84	**1.84***	**1.88***	1.79	1.79	1.77	1.75	1.73	1.71	1.66
average	1.77	1.82	1.84	1.87	1.88	1.88	1.91	1.92	1.93	1.90	1.90	1.88	1.84	1.82	1.77	1.74

* The area that radiation dose measurement by TLD was made.

b) For 12 MeV (Continued).

Distance from cone end	**Collimator angle related to the point on the surface of IORT cone**															
	180°	192°	204°	216°	228°	240°	252°	264°	270°	276°	288°	300°	312°	324°	336°	348°
8 cm	1.78	1.74	1.68	1.63	1.58	1.55	1.57	1.53	1.53	1.53	1.55	1.57	1.61	1.68	1.74	1.78
7 cm	1.75	1.73	1.64	1.60	1.56	1.53	1.55	1.52	1.52	1.51	1.52	1.55	1.60	1.66	1.72	1.76
6 cm	1.73	1.68	1.62	1.59	1.55	1.53	1.51	1.49	1.48	1.48	1.50	1.54	1.59	1.64	1.70	1.75
5 cm	1.71	1.66	1.60	1.57	1.52	1.52	1.50	1.47	1.47	1.47	1.49	1.53	1.56	1.63	1.68	1.74
4 cm	1.69	1.64	1.58	1.54	1.48	1.50	1.50	1.47	1.46	1.46	1.48	1.50	1.55	1.61	1.66	1.71
3 cm	1.65	1.62	1.56	1.52	1.47	1.46	1.46	1.46	1.46	1.45	1.45	1.45	1.52	1.59	1.64	1.69
2 cm	1.64	1.59	1.54	1.51	1.47	1.47	1.43	1.43	1.44	1.44	1.40	1.45	1.49	1.56	1.62	1.67
1 cm	1.63	1.58	1.53	1.48	1.45	1.45	1.44	1.46	1.40	1.38	1.42	1.45	1.45	1.55	1.60	1.65
0 cm	1.61	1.55	1.50	1.41	1.45	1.44	1.45	1.47	1.39	1.35	1.42	1.40	1.39	1.49	1.53	1.58
average	1.69	1.64	1.58	1.54	1.50	1.49	1.49	1.48	1.46	1.45	1.47	1.49	1.53	1.60	1.65	1.70

* The area that radiation dose measurement by TLD was made.

c) For 20 MeV.

Distance from cone end	Collimator angle related to the point on the surface of IORT cone															
	0°	12°	24°	36°	48°	60°	72°	84°	90°	96°	108°	120°	132°	144°	156°	168°
8 cm	1.97	2.04	2.09	2.14	2.15	2.14	**2.16***	**2.17***	2.04	2.02	2.02	2.00	2.02	2.00	1.98	1.96
7 cm	1.94	2.02	2.05	2.11	2.13	2.14	2.15	2.16	2.03	2.02	2.02	2.00	2.01	1.99	1.99	1.97
6 cm	1.90	1.98	2.03	2.09	2.10	2.12	**2.14***	**2.14***	2.03	2.03	2.02	2.01	2.00	1.99	1.99	1.97
5 cm	1.87	1.95	2.00	2.06	2.07	2.08	2.12	2.12	2.03	2.03	2.01	2.01	2.00	2.00	1.98	1.95
4 cm	1.83	1.91	1.97	2.03	2.05	2.03	**2.10***	**2.08***	2.01	2.02	2.01	2.00	1.99	1.99	1.97	1.95
3 cm	1.80	1.90	1.94	1.99	2.02	2.01	2.05	2.05	2.00	2.00	2.00	2.00	1.99	1.98	1.96	1.94
2 cm	1.78	1.85	1.90	1.96	2.00	1.99	**2.02***	**2.03***	2.00	1.99	1.99	1.99	1.98	1.98	1.95	1.93
1 cm	1.71	1.84	1.89	1.95	1.97	1.96	1.99	1.99	1.99	1.99	1.99	1.99	1.98	1.96	1.93	1.90
0 cm	1.65	1.79	1.85	1.91	1.92	1.91	**1.98***	**1.98***	1.97	1.90	1.92	1.98	1.92	1.89	1.87	1.85
average	1.83	1.92	1.97	2.03	2.05	2.04	2.08	2.08	2.00	2.00	2.00	2.00	1.99	1.98	1.96	1.94

* The area that radiation dose measurement by TLD was made.

c) For 20 MeV (Continued).

Distance from cone end	Collimator angle related to the point on the surface of IORT cone															
	180°	192°	204°	216°	228°	240°	252°	264°	270°	276°	288°	300°	312°	324°	336°	348°
8 cm	1.95	1.90	1.84	1.81	1.75	1.73	1.70	1.65	1.62	1.59	1.63	1.65	1.68	1.75	1.81	1.88
7 cm	1.94	1.89	1.84	1.79	1.74	1.71	1.67	1.63	1.60	1.58	1.60	1.65	1.66	1.72	1.78	1.85
6 cm	1.93	1.88	1.82	1.77	1.72	1.69	1.65	1.61	1.57	1.55	1.59	1.60	1.63	1.70	1.74	1.82
5 cm	1.91	1.87	1.81	1.73	1.71	1.68	1.63	1.59	1.56	1.53	1.54	1.60	1.63	1.67	1.71	1.79
4 cm	1.91	1.86	1.79	1.72	1.66	1.65	1.62	1.57	1.53	1.51	1.54	1.56	1.58	1.63	1.67	1.75
3 cm	1.89	1.83	1.76	1.71	1.66	1.60	1.59	1.55	1.52	1.50	1.51	1.52	1.58	1.59	1.63	1.71
2 cm	1.87	1.80	1.71	1.69	1.62	1.59	1.55	1.53	1.51	1.50	1.48	1.49	1.54	1.58	1.61	1.69
1 cm	1.86	1.77	1.67	1.61	1.57	1.58	1.54	1.51	1.50	1.49	1.49	1.44	1.54	1.56	1.52	1.62
0 cm	1.80	1.74	1.68	1.61	1.53	1.51	1.53	1.50	1.49	1.49	1.48	1.44	1.48	1.50	1.48	1.56
average	1.90	1.84	1.77	1.72	1.66	1.64	1.61	1.57	1.54	1.53	1.54	1.55	1.59	1.63	1.66	1.74

* The area that radiation dose measurement by TLD was made.

Table IX. The depth of maximum dose in water phantom of IORT cone diameters 4.5, 6.4, 8.3 and 9.5 cm for the electron beam energies of 6, 12 and 20 MeV both flat and 30° beveled ends.

Cone type	Cone diameter (cm)	Energy		
		6 MeV	12 MeV	20 MeV
Flat end	4.5	1.3	2.4	2.3
	6.4	1.3	2.8	2.7
	8.3	1.3	2.5	2.5
	9.5	1.3	2.8	2.8
30° Beveled end	4.5	0.8	1.5	2.1
	6.4	0.8	1.8	2.4
	8.3	0.8	1.9	2.4
	9.5	0.8	1.9	2.0

Table X The maximum radiation leakage in the percentage of the dose at d_{max} of IORT cone measured by the TLDs.

Cone diameter (cm)	Distance from cone end (cm)	Flat end			Distance from cone end (cm)	30° bevel end		
		6 MeV	12 MeV	20 MeV		6 MeV	12 MeV	20 MeV
		dose(%)±SD	dose(%)±SD	dose(%)±SD		dose(%)±SD	dose(%)±SD	dose(%)±SD
4.5	8	5.01 ± 0.07	7.66 ± 0.31	13.10 ± 0.30	8	6.18 ± 0.33	9.44 ± 0.46	18.13 ± 0.26
	6	4.79 ± 0.16	7.61 ± 0.23	12.42 ± 0.24	6	5.83 ± 0.26	9.09 ± 0.32	16.70 ± 0.78
	4	4.57 ± 0.04	7.55 ± 0.15	11.73 ± 0.26	4	5.45 ± 0.20	8.46 ± 0.26	15.28 ± 0.33
	2	4.47 ± 0.09	7.22 ± 0.06	11.28 ± 0.32	2	5.15 ±0.65	7.90 ± 0.33	14.05 ± 0.42
	0	4.37 ± 0.13	6.88 ± 0.12	10.82 ± 0.51	0	4.92 ± 0.14	7.41 ± 0.28	13.00 ± 0.62
6.4	8	6.26 ± 0.09	10.98 ± 0.21	17.45 ± 0.17	8	6.88 ± 0.28	11.95 ± 0.10	18.94 ± 0.29
	6	6.06 ± 0.24	10.45 ± 0.12	16.85 ± 0.16	6	6.81 ± 0.25	11.78 ± 0.27	17.74 ± 0.22
	4	5.85 ± 0.10	9.92 ± 0.14	16.24 ± 0.34	4	6.74 ± 0.26	11.60 ± 0.19	16.53 ± 0.13
	2	5.73 ± 0.30	9.55 ± 0.09	15.56 ± 0.26	2	6.66 ± 0.12	11.28 ± 0.18	15.85 ± 0.20
	0	5.60 ± 0.34	9.17 ± 0.28	14.88 ± 0.30	0	6.58 ± 0.19	10.96 ± 0.26	15.15 ± 0.17
8.3	8	7.89 ± 0.23	12.44 ± 0.30	22.94 ± 0.11	8	8.38 ± 0.16	14.37 ± 0.25	***23.10 ± 0.12**
	6	7.47 ± 0.12	11.71 ± 0.24	21.63 ± 0.25	6	7.95 ± 0.22	13.47 ± 0.13	22.02 ± 0.18
	4	7.04 ± 0.23	10.97 ± 0.28	20.31 ± 0.29	4	7.52 ± 0.25	11.91 ± 0.24	20.94 ± 0.25
	2	6.65 ± 0.19	10.24 ± 0.19	19.55 ± 0.31	2	7.18 ± 0.13	11.01 ± 0.26	19.86 ± 0.29
	0	6.25 ± 0.39	9.50 ± 0.39	18.78 ± 0.49	0	6.93 ± 0.16	10.56 ± 0.28	18.66 ± 0.36
9.5	8	7.45 ± 0.25	10.97 ± 0.32	19.20 ± 0.49	8	8.84 ± 0.06	13.60 ± 0.29	21.33 ± 0.24
	6	7.20 ± 0.22	10.58 ± 0.22	18.65 ± 0.35	6	8.28 ± 0.17	13.03 ± 0.53	20.70 ± 0.30
	4	6.95 ± 0.07	10.19 ± 0.24	18.10 ± 0.32	4	7.72 ± 0.13	12.46 ± 0.46	20.07 ± 0.26
	2	6.43 ± 0.21	9.86 ± 0.19	17.39 ± 0.24	2	7.44 ± 0.18	11.76 ± 0.48	19.15 ± 0.23
	0	5.91 ± 0.41	9.53 ± 0.28	16.68 ± 0.64	0	6.87 ± 0.15	11.40 ± 0.33	18.14 ± 0.41

* The maximum value.

a)

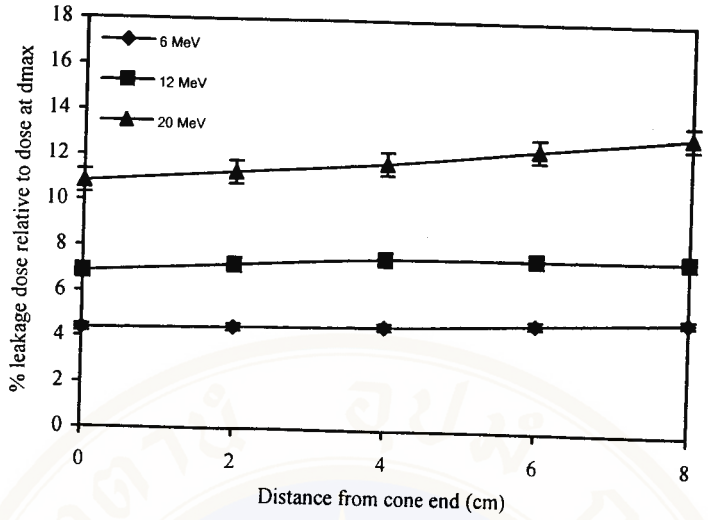

b)

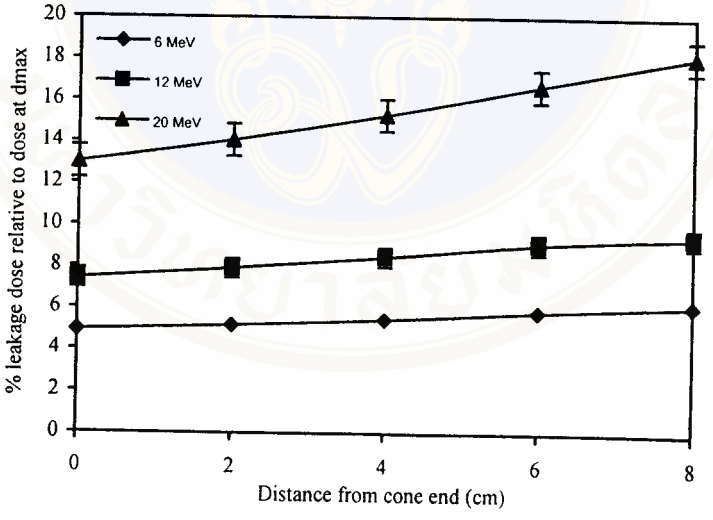

Figure 26. The percent of maximum radiation leakage related to the dose at the depth of maximum dose as a function of the distance (cm) from cone end for 4.5 cm diameter cone with : a) flat end b) bevel end.

a)

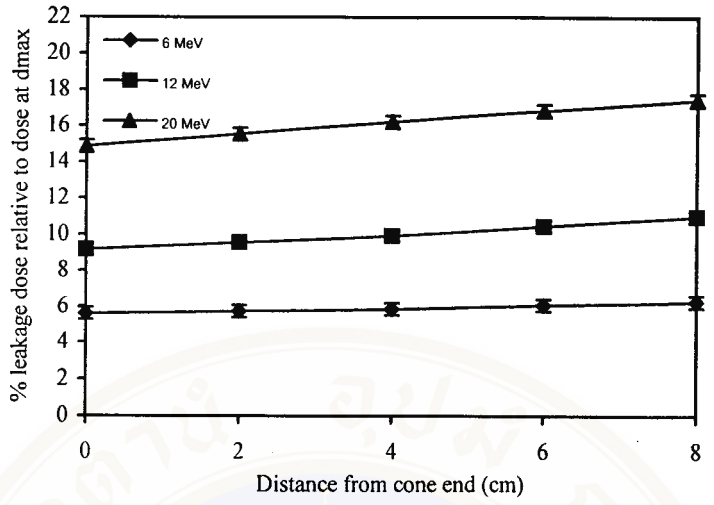

b)

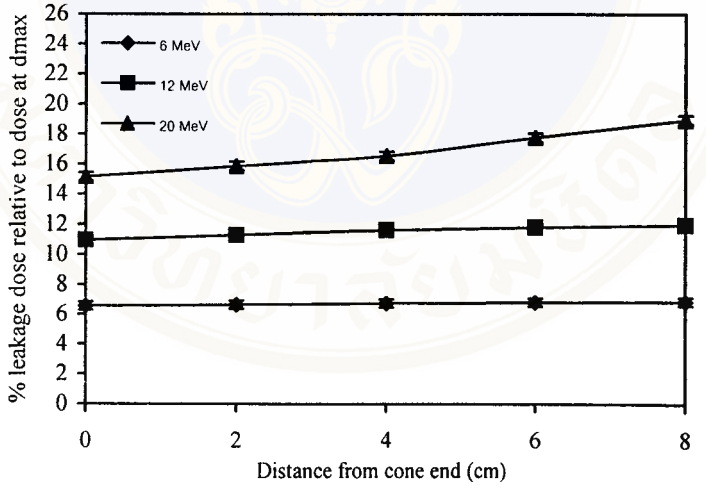

Figure 27. The percent of maximum radiation leakage related to the dose at the depth of maximum dose as a function of the distance (cm) from cone end for 6.4 cm diameter cone with : a) flat end b) bevel end.

a)

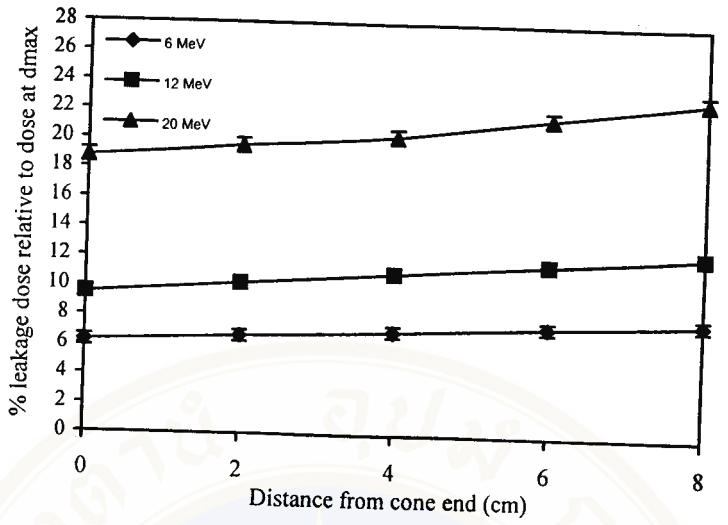

b)

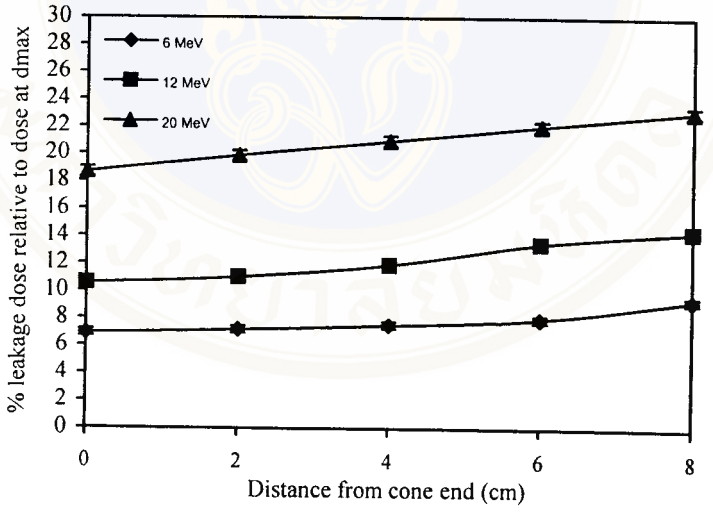

Figure 28. The percent of maximum radiation leakage related to the dose at the depth of maximum dose as a function of the distance (cm) from cone end for 8.3 cm diameter cone with : a) flat end b) bevel end.

a)

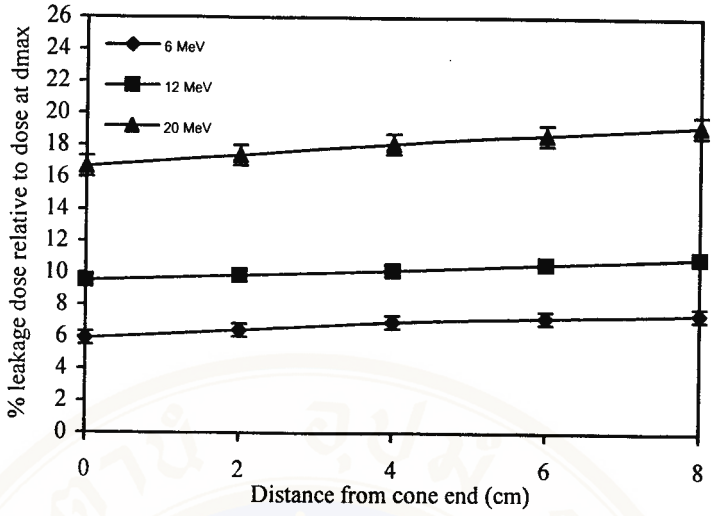

b)

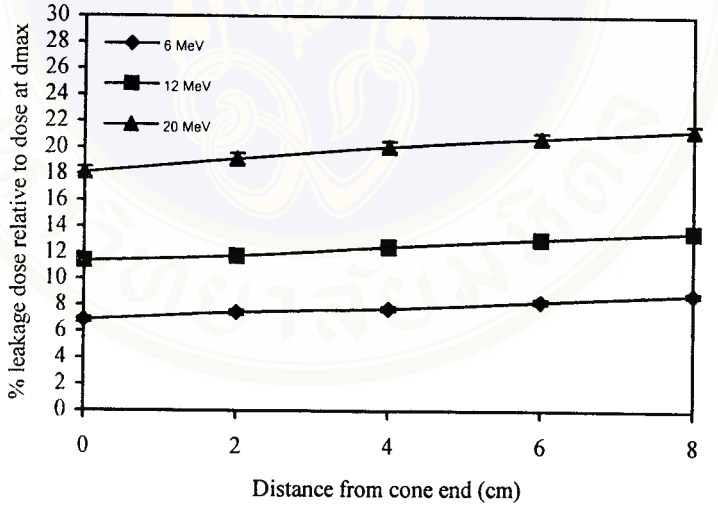

Figure 29. The percent of maximum radiation leakage related to the dose at the depth of maximum dose as a function of the distance (cm) from cone end for 9.5 cm diameter cone with : a) flat end b) bevel end.

Table XI. The leakage dose at the distance of 4 cm from the cone end in the percentage of the value at d_{max} for the various sizes of the cones and energies.

Cone diameter (cm)	Leakage dose relative to dose at d_{max} (%)					
	Flat end			Bevel end		
	6 MeV	12 MeV	20 MeV	6 MeV	12 MeV	20 MeV
4.5	4.57	7.55	11.73	5.45	8.46	15.28
6.4	5.85	9.92	16.24	6.74	11.60	16.53
8.3	7.04	10.97	20.31	7.52	11.91	**20.94***
9.5	6.95	10.19	18.10	7.72	12.46	20.07

* The maximum value.

Table XII. The leakage dose at the distance of 4 cm from the cone end as the percentage of the tumor dose at the treatment depth of 90% isodose.

Cone diameter (cm)	Leakage dose relative to dose at d_{max} (%)					
	Flat end			Bevel end		
	6 MeV	12 MeV	20 MeV	6 MeV	12 MeV	20 MeV
4.5	5.08	8.39	13.03	6.06	9.40	16.98
6.4	6.50	11.02	18.04	7.49	12.89	18.37
8.3	7.82	12.19	22.56	8.36	13.23	**23.27***
9.5	7.72	11.32	20.11	8.58	13.84	22.30

* The maximum value.

CHAPTER VI

DISCUSSION

Since the abdominal tumor is most frequently treated by the IORT which the normal tissues normally involved are gastrointestinal, colorectal, kidney, and liver. As proposed by Perez and Brady (41), the gastrointestinal is the least tolerant organ with the tolerance dose ($TD_{5/5}$-$TD_{50/5}$) of 5-10 Gy. The tolerance doses, $TD_{5/5}$-$TD_{50/5}$ are the doses inducing the radiation complication in 5 years with the chance of 5 % and 50 % respectively. According to this study, the normal tissue of the patient treated by our IORT system should not receive the radiation dose of more than 23.27 % of the tumor dose because 4 cm is the largest distance for the normal tissues to extend along the cone wall. For the abdominal tumor normally treated by 10-20 Gy, the normal tissue should not receive more than 4.65 Gy. It would seem to appear that : (1) the normal tissues should receive less than $TD_{5/5}$ of 5 Gy, (2) the tolerance doses for the normal tissues should be more than the proposed values since they are for the whole organ irradiation but normally only partial volume of the organ is involved. For the hard docking applicator system used in this study, the radiation leakage outside the treatment field can be reduced by using a lead sheet surrounding the tip of the cone (42). With a soft docking system, a shielding plate with 2 mm Pb and 1.5 mm Al was added on the top of the cone to reduce the leakage dose outside the cone wall to be less than 5 % (23).

CHAPTER VII

CONCLUSION

In the radiation treatment by IORT, the radiation leakage outside the treatment field is very important since a large dose is delivered to the tumor in a single fraction. The leakage dose has to be determined at the end of the cones and also along the wall of the cones. Normal tissues variably extend upto some height along the wall of the cone. Although it is convenient and capable in using film to search for the maximum leakage area around the outside wall of the cone, but TLD is more suitable to determine the leakage dose in the percentage of the maximum dose in phantom (at d_{max}). If films are used to measure the doses outside and inside the treatment field with a single irradiation, the optical density on these two films will be much different that one of them may be out of the readable range. It is found from this study that the leakage radiation increased with increasing energy and cone size but it is more dependent of the energy. The cone 8.3 cm showed more leakage radiation than the 9.5 cm cone. This may be due to the scattered radiation and bremsstrahlung occurred in the brass plate on the top of the 8.3 cm cone. Since the 9.5 cm cone has the same diameter as the applicator attachment, it does not need an additional collimation (brass plate). Every bevel end cone showed higher leakage dose than the flat one with the maximum value of 3.95% (relative to tumor dose) from the smallest cone (4.5 cm) with the highest energy (20 MeV).

In conclusion, not only the beam data for an IORT, but also the leakage dose outside the cone have to be individually determined for each applicating system, cone size, energy and machine. For the IORT in Ramathibodi Hospital, the dose to a critical organ can be determined directly by using the data in Table X, although if should not be more than the limit.

REFERENCES

1. Abe M, Takahashi M, Yabumoto E, et al. Techniques, indications and results of intraoperative radiation therapy of advanced cancers. Radiology. 1975; 116, 693.
2. Rich TA, Cady B, and Mcdermotl WV. Orthovoltage intraoperative radiotherapy : A new look at an old idea. Int J Radiat Oncol Biol Phys. 1984; 10 : 1957.
3. Biggs PJ, Epp ER, Ling CC, Novack DH, and Michels HB. Dosimetry, field shaping and other considerations for intraoperative electron therapy. Int J Radiat Oncol Biol Phys. 1981; 7 : 875-84.
4. Frass BA, Miller RW, Kinsella TJ, et al. Int J Radiat Oncol Biol Phys. 1985; 11 : 1299-311.
5. Palta JR, Biggs PJ, Hazel JD, et al. Intraoperative electron beam radiation therapy : Technique, dosimetry, and dose specification : Report of Task Force 48 of the Radiation therapy Committee, American Association of Physicist in Medicine. Int J Radiat Oncol Biol Phys. 1995; 33 : 725-46.
6. Bagne FR, Dobelbower RR, Milligan AJ, and Bronn DG. Treatment of cancer of the pancreas by intropeative electron beam therapy : Physical and biological aspects. Int J Radiat Oncol Biol Phys. 1989; 16 : 231-42.
7. Dobelbower RR and Abe M. History of intraoperative radiation therapy. In : Intraoperative Radiation Therapy. Florida : CRC Press; 1989 : 1-9.
8. Khan FM. Clinical radiation generators. In : The Physics of Radiation Therapy. 2nd ed. Baltimore : William & Wilkins; 1994 : 51-8.

9. John HE, Cunningham JR. High energy machines. In : The physics of Radiology. 4 th ed. Illinois : Charles C Thomas; 1983 : 108-18.

10. Klevenhagen SC. Electron interactions with matter. In : Physics of electron beam, Medical Physics Handbooks 13 Bristol : Adam Hilger Ltd, 1985 : 37-66.

11. Klevenhagen SC. Scattering collisions. In : Physics and dosimetry of therapy electron beams. Wisconsin : Medical Physics Publishing, 1993 : 52-78.

12. Klevenhagen SC. Radiation quality of electron beam. In : Physics of electron beam, Medical Physics Handbooks 13. Bristol : Adam Hilger Ltd, 1985 : 61-6.

13. Williams JR, Thwaites DI. Beam characteristics. In : Radiotherapy physics in practice. New York : Oxford University Press; 1993 : 174-6.

14. Klevenhagen SC. Range-energy relationship. In : Physics and dosimetry of therapy electron beams. Wisconsin : Medical Physics Publishing, 1993 : 121-3.

15. Dobelbower RR, Abe M. Physical aspects of intraoperative radiation therapy. In : Intraoperative Radiation Therapy. Florida : CRC Press. 1989 : 59-74.

16. Khan FM. Isodose curve. In : The Physics of Radiation Therapy. 2nd ed. Baltimore : William & Wilkins, 1994 : 365-6.

17. International Commission on Radiation Units and Measurement. Radiation dosimetry : electron beams with energies between 1 and 50 MeV. ICRU report 35; 1984 : 110-1.

18. Khan FM, Doppke K, Hogstrom KR, et al. Clinical electron beam dosimetry. Report of AAPM Radiation Therapy Committee Task Group No. 25. Med Phys 1991; 18 : 73.

19. Knoos T, Weber L, Larsson K, Nilsson P, and Graffman S. An intraoperative radiotherapy soft docking system for an SL 25 accelerator. In : International radiotherapy review. UK : Philips Medical Systems. 1995 : 127-47.

20. Jones D, Taylor E, Travaglini J, and Vermeulen S. A non-contacting intraoperative electron cone apparatus. Int J Radiation Oncology Biol. Phys. 1989; 16, 1643-47.

21. Radiation products design. Model 1100-00 intraoperative periscopic electron cone system. USA; Radiation products design.

22. Hogstrom KR, Boyer AL, Shiu AS, et al. Design of metallic electron beam cones for an intraoperative therapy linear accelerator. Int. J. Radiation oncology Biol. Phys. 1990; 18, 1223-32.

23. Kharrati H, Aletti P, and Guillemin F. Design of an non-docking intraoperative electron beam applicator system. Radiation therapy and Oncology. 1994; 33, 80-3.

24. Dobelbower RR, Abe M. Physical aspects and dosimetric considerations for intraoperative radiation therapy with electron beam. In : Intraoperative Radiation Therapy. Florida : CRC Press. 1989 : 35-58.

25. Bagne FR, Samsami N, and Dobellower RR. Radiation contamination and leakage assessment of Intraoperative electron applicators. Med Phys. 1988; 15, 530-537.

26. McCullough EC and Anderson JA. The dosimetric properties of an applicator system for intraoperative electron-beam therapy utilizing a Clinac-18 accelerator. Med Phys. 1982; 9(2), 261-7.

27. Khan FM. Thermoluminescence dosimetry. In : The Physics of Radiation Therapy. 2nd ed. Baltimore : William & Wilkins, 1984 : 148-53.

28. Mickinley AF. Lithium Fluoride In : Medical physics handbooks 5 : Thermoluminescent dosimetry. Brystal : Adam Hilger LTD, 1981 : 32-7.

29. John HE, Cunningham JR. Thermoluminescent dosimetry. In : The physics of Radiology. 4 th ed. Illinois : Charles C Thomas, 1983 : 317-9.

30. Khan FM. Film dosimetry. In : The Physics of Radiation Therapy. 2nd ed. Baltimore : William & Wilkins, 1994 : 172-3.

31. Klevenhagen SC. Film characterisrics. In : Physics and dosimetry of therapy electron beams. Wisconsin : Medical Physics Publishing, 1993 : 374-81.

32. Attix FH. Optical density of film. In : Introduction to radiological physics and radiation dosimetry. USA : John Wiley & Sons. 1986 : 412-4.

33. Palta JR, and Suntharalingam N. A non-docking intraoperative electron beam applicator system. Int. J. Radiation Oncology Biol. Phys. 1989; 17, 411-417.

34. Varian Associates. Varian Radiation Oncology Systems, 2100C Clinac. USA : Varian Associates, 1991.

35. Varian Associates. Varian Radiation Therapy Systems, 2100C Clinac. USA : Varian Associates, 1991.

36. Scanditronix. RFA-300 Radiation Field Analyzer Manual Software Version 4.2. Sweden ; 1992.

37. Harshaws Bicron. Instruction Manual for TLD oven, Saint Gobain/Norton Industrial Ceremics Co., Ohio 1993.

38. Harshaw Bicron. Automatic TLD Reader User's Manual, Saint Gobain/Norton Industrial Ceremics Co., Ohio 1993.

39. Khan FM. Dose distribution and scatter analysis. In : The Physics of Radiation Therapy. 2nd ed. Baltimore : William & Wilkins, 1994 : 176-199.

40. John HE, Cunningham JR. Measurement of radiation dosimetry. In : The physics of Radiology. 4th ed. Illinois : Charles C Thomas, 1983 : 237-248.

41. Perez CA, Brady LW. Late effects of cancer treatment. In : Principles and Practice of Radiation oncology. 3rd ed. Philadelphia : Lippincott-Raven Publishers, 1998 : 155-211.

42. Papanikolaou N, Paliwal B. A study of the effect of cone shielding in intraoperative radiotherpy. Med Phys. 1995; 22(5), 571-5.

BIOGRAPHY

NAME Mr. Choengchai Orkongkiat

DATE OF BIRTH 5 May 1972

PLACE OF BIRTH Bangkok, Thailand

INSTITUTIONS ATTENDED Mahidol University , 1990-1994 :
Bachelor of Science (Radiological Technology)
Mahidol University , 1996-1998 :
Master of Science (Medical Physics)

POSITION & OFFICE 1999 - Present, Dept. of Radiology
Faculty of Medicine, Ramathibodi Hospital, Bangkok, Thailand.
Position : Radiation Technologist.